

Childhood Cancer Data Initiative Webinar Series

# The Mutational Epidemiology of Childhood Cancer

*Logan Spector, Ph.D.*

# Today's Speaker



## Logan Spector, Ph.D.

Professor and Director  
Division of Epidemiology and Clinical Research  
Department of Pediatrics  
University of Minnesota

# The Many Meanings of “Mutation” (Part 1)



Low frequency,  
often pathogenic,  
germline variant  
(outdated)

*De novo* variant at  
conception (a.k.a.  
*de novo* mutation  
or DNM)

Somatic variant  
present in tumor  
but not normal  
tissue

# The Many Meanings of “Mutation” (Part 2)



Low frequency,  
often pathogenic,  
germline variant  
(outdated)

*De novo* variant at  
conception (a.k.a.  
*de novo* mutation  
or DNM)

Somatic variant  
present in tumor  
but not normal  
tissue

# Drivers and Passengers in Cancer

## Passengers:

Along for the ride, not necessary to get cells moving, but might affect the driver if rowdy



## Drivers:

Gets the cell moving by stepping on the gas and keeping off the brakes

# Cancer Driver Mutations: Predications and Reality

Review

## Cancer driver mutations: predictions and reality

Daria Ostroverkhova,<sup>1</sup> Teresa M. Przytycka,<sup>2,\*</sup> and Anna R. Panchenko<sup>1,2,4,5,6</sup>

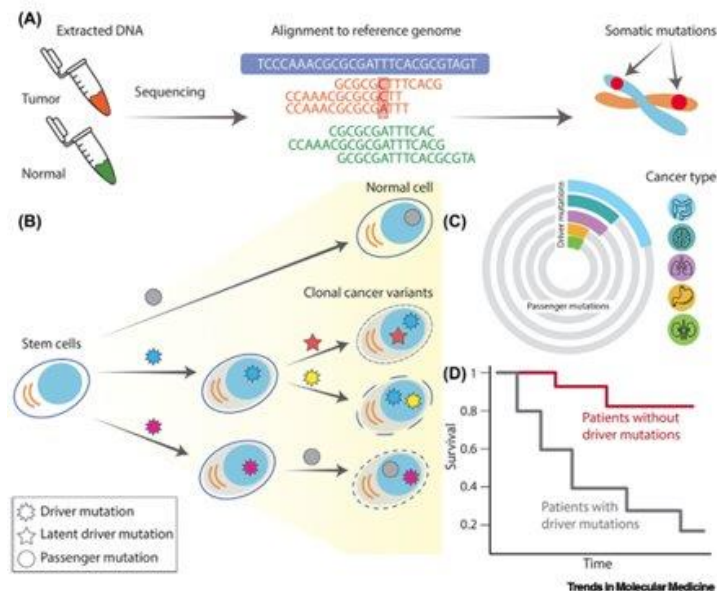
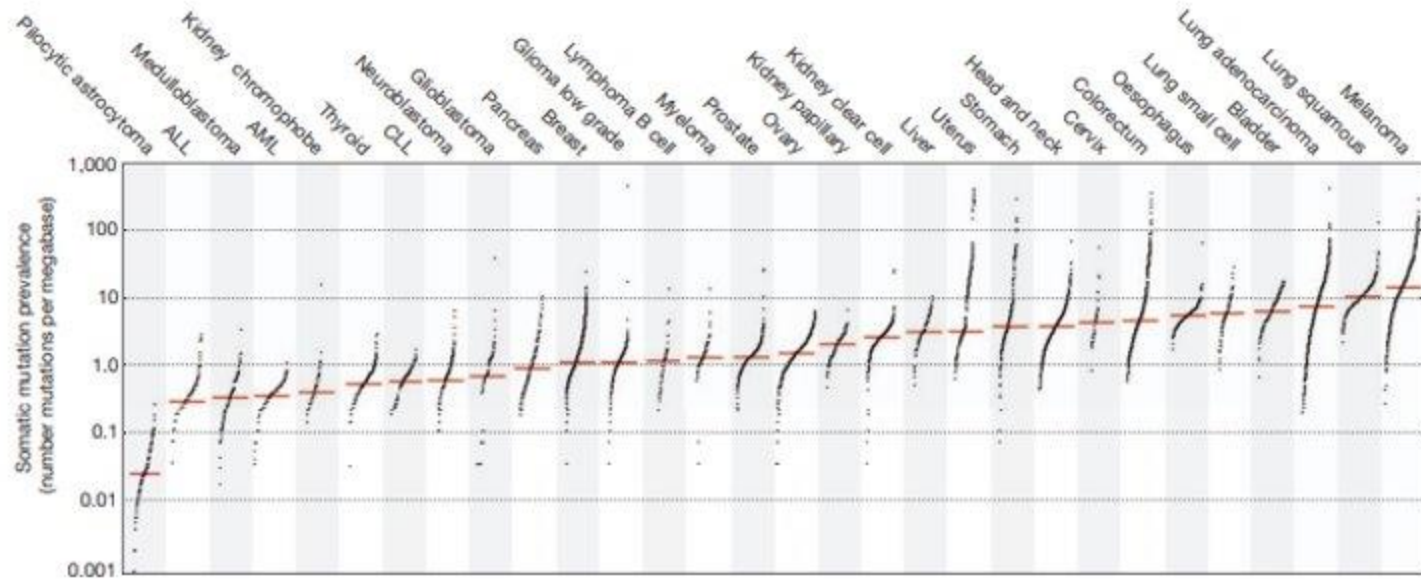


Figure 1. Driver and passenger mutations in human cancer. (A) Detection of somatic mutations in human cancers requires the extraction of DNA from tumor and normal samples, DNA sequencing, and alignment of paired tumor-normal sequences to the human reference genome for subsequent mutation calling. (B) Cancerogenesis is a multistage process in which cells accumulate a myriad of somatic mutations throughout their life. Driver mutations lead to a variety of genetic and epigenetic alterations that are beneficial to cancer cells. (C) The proportion of driver mutations per cancer type: all mutations are shown in gray radial bars, colored radial bars correspond to driver mutations for each cancer type. (D) In some cancer types, patients harboring driver mutations are characterized by better or worse survival compared to patients without drivers, underlining the clinical importance of driver mutation identification.

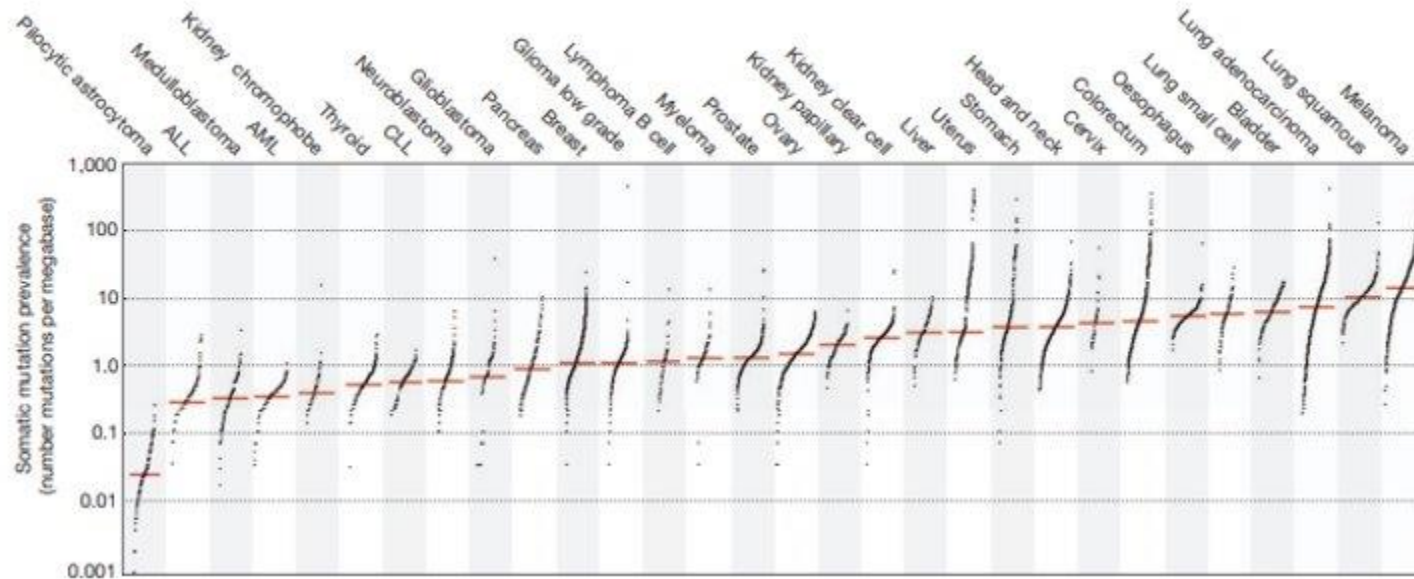
# Signatures of Mutational Processes in Human Cancer (Part 1)



# Signatures of Mutational Processes in Human Cancer (Part 2)



Ludmil Alexandrov



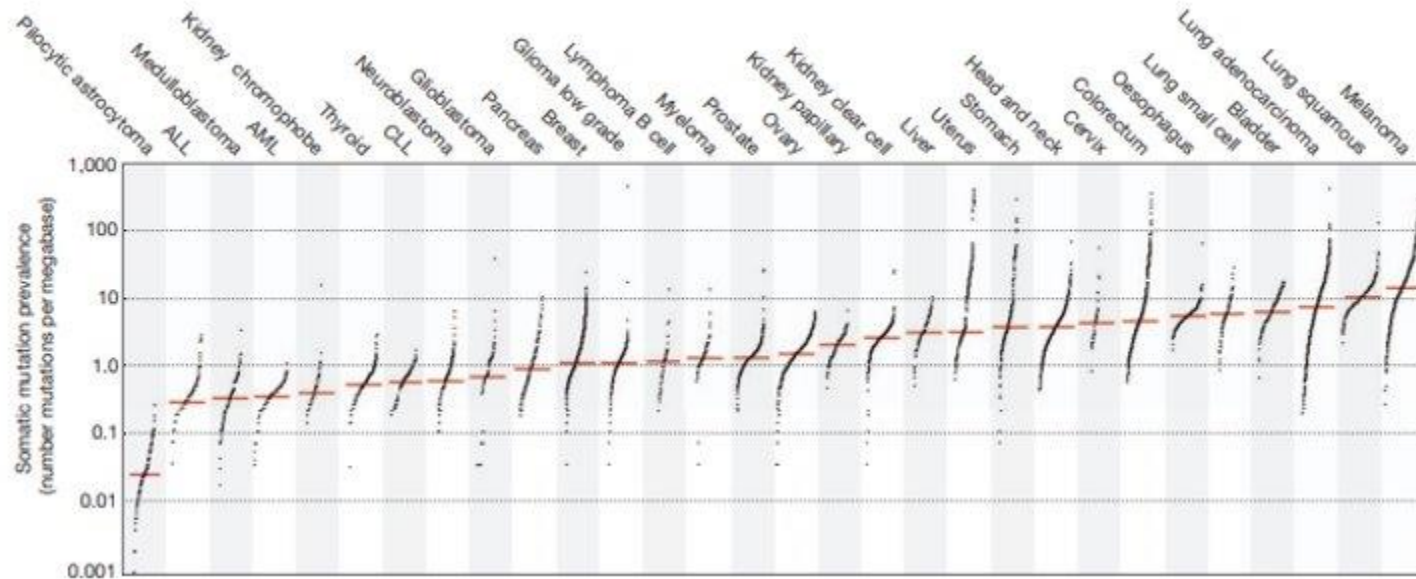


# Signatures of Mutational Processes in Human Cancer (Part 3)

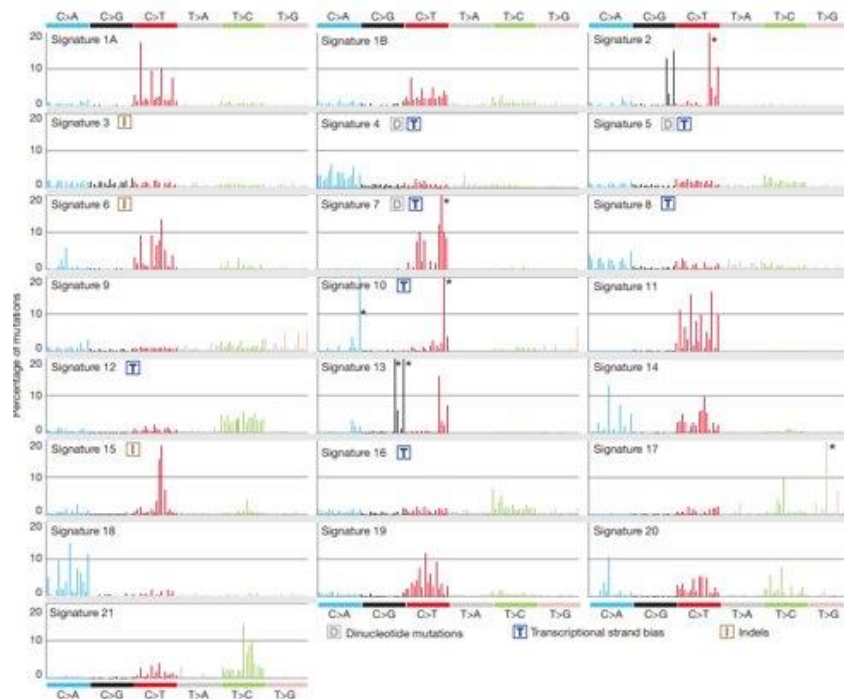


“mutSig”

Ludmil Alexandrov



# Signatures of Mutational Processes in Human Cancer (Part 4)



**Figure 2 | Validated mutational signatures found in human cancer.** Each signature is displayed according to the 96 substitution classification defined by the substitution class and sequence context immediately 3' and 5' to the mutated base. The probability bars for the six types of substitutions are displayed in different colours. The mutation types are on the horizontal axes.

whereas vertical axes depict the percentage of mutations attributed to a specific mutation type. All mutational signatures are displayed on the basis of the trinucleotide frequency of the human genome. A higher resolution of each panel is found respectively in Supplementary Figs 2-23. Asterisk indicates mutation type exceeding 20%.

# Signatures of Mutational Processes in Human Cancer (Part 5)



**Figure 3 | The presence of mutational signatures across human cancer types.** Cancer types are ordered alphabetically as columns whereas mutational signatures are displayed as rows. 'Other' indicates mutational signatures for which we were not able to perform validation or for which validation failed (Supplementary Figs 24–28). Prevalence in cancer samples indicates the

percentage of samples from our data set of 7,042 cancers in which the signature contributed significant number of somatic mutations. For most signatures, significant number of mutations in a sample is defined as more than 100 substitutions or more than 25% of all mutations in that sample. MMR, mismatch repair.

# Mutational Signatures



**COSMIC** **Wellcome Sanger Institute**

Human Cancer Signatures Experimental Signatures Analysis Tools COSMIC Downloads

Human Cancer v3.4 Experimental v1.0

## Mutational Signatures

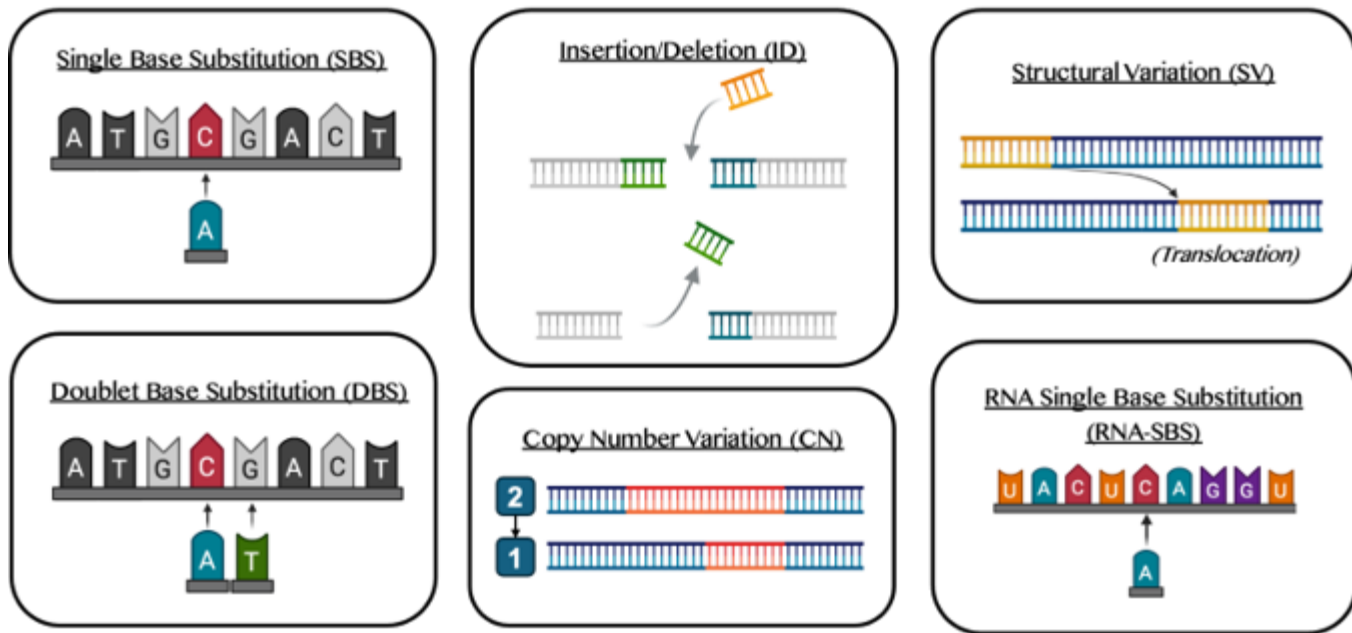
Pioneering techniques to understand the causes of cancer. Mutagenic compounds leave characteristic patterns of damage throughout our genome. Each one creates a unique and distinctive pattern of damage. These patterns are Mutational Signatures. This website is here to share our data and tools so that together, we can cure cancer, faster.

[SigProfilerAssignment](#) [Learn More](#)

CANCER GRAND CHALLENGES Wellcome Sanger Institute COSMIC

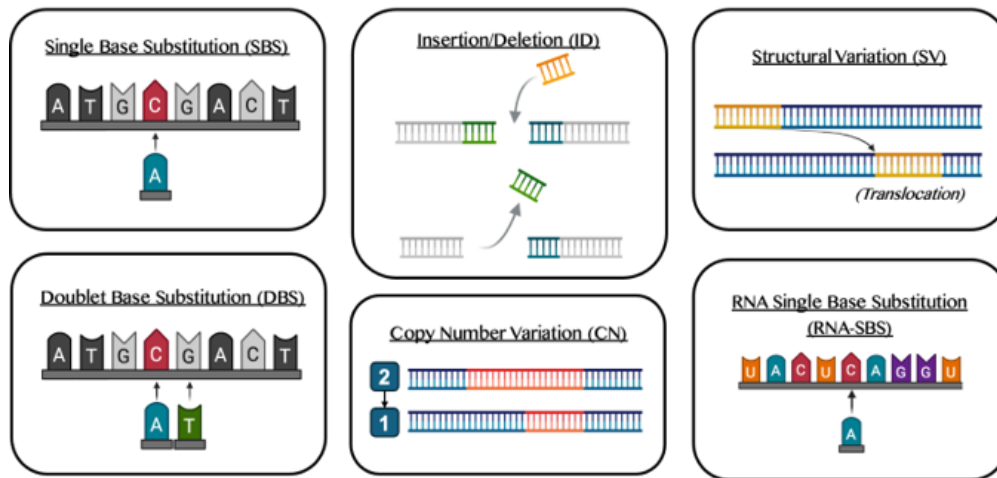
# COSMIC Mutational Signatures (Part 1)

## COSMIC Mutational Signatures



# COSMIC Mutational Signatures (Part 2)

## COSMIC Mutational Signatures



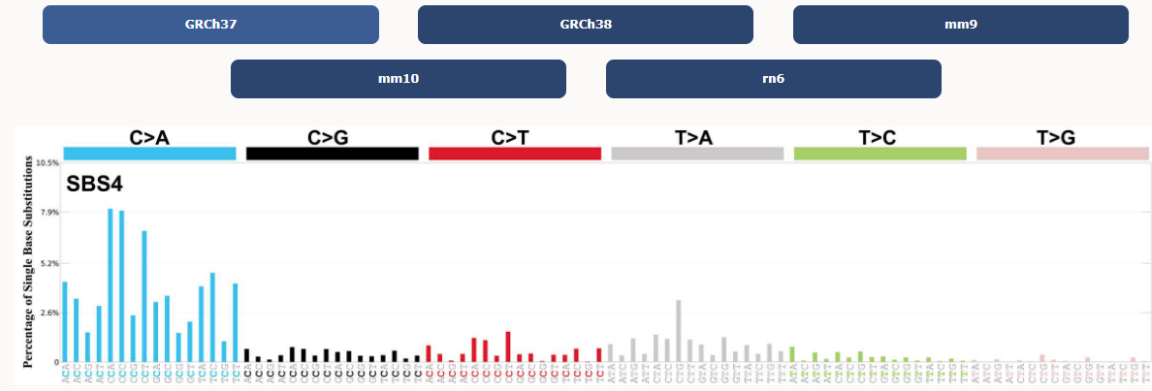
COSMIC release v3.4:

SBS: 96  
DBS: 78  
ID: 83  
CN: 48  
RNA-SBS: 192  
SV: 32

## Mutational Signatures (v3.4 - October 2023)

### SBS4 · GRCh37 · COSMIC v102

#### Mutational profile



#### Proposed aetiology

Associated with tobacco smoking. Its profile is similar to the mutational spectrum observed in experimental systems exposed to tobacco carcinogens such as benzo[a]pyrene. SBS4 is, therefore, likely due to direct DNA damage by tobacco smoke mutagens.

#### Comments

Although tobacco smoking causes multiple cancer types in addition to lung and head and neck, SBS4 has not been detected in many of these. [SBS29](#) is found in cancers associated with tobacco chewing and appears different from SBS4.



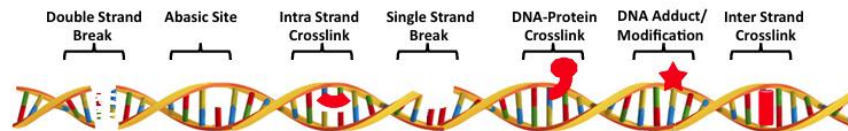
# Investigating the origins of the mutational signatures in cancer (part 1)

## Investigating the origins of the mutational signatures in cancer

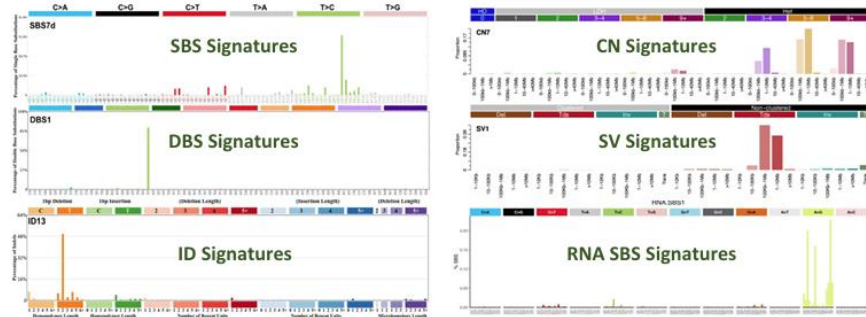
Gunnar Boysen <sup>1,2,\*</sup>, Ludmil B. Alexandrov <sup>3,\*</sup>, Raheleh Rahbari <sup>4</sup>, Intawat Nookaew <sup>5</sup>,  
Dave Ussery <sup>5</sup>, Mu-Rong Chao <sup>6,7</sup>, Chiung-Wen Hu <sup>8</sup> and Marcus S. Cooke <sup>9,10,\*</sup>



### DNA Adductome



### Mutational Signatures

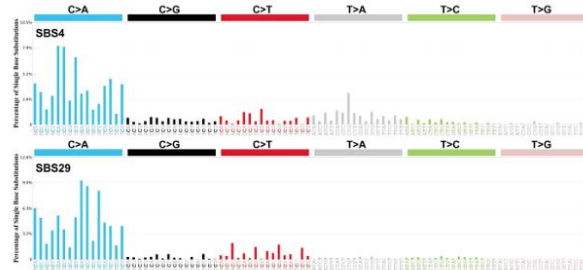




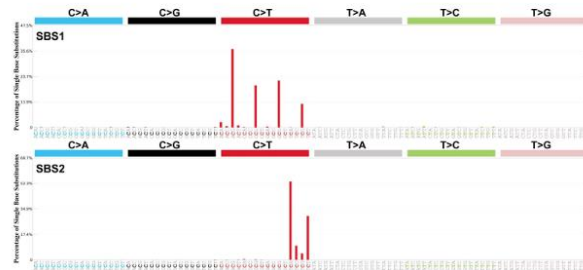
# Investigating the origins of the mutational signatures in cancer (part 2)

## Investigating the origins of the mutational signatures in cancer

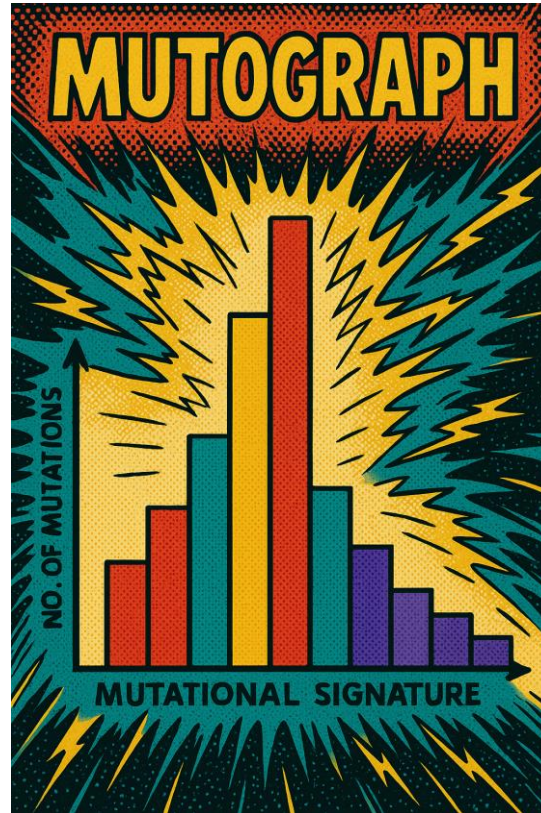
Gunnar Boysen <sup>1,2,\*</sup>, Ludmil B. Alexandrov <sup>3,\*</sup>, Raheleh Rahbari <sup>4</sup>, Intawat Nookaew <sup>5</sup>,  
Dave Ussery <sup>5</sup>, Mu-Rong Chao <sup>6,7</sup>, Chiung-Wen Hu <sup>8</sup> and Marcus S. Cooke <sup>9,10,\*</sup>



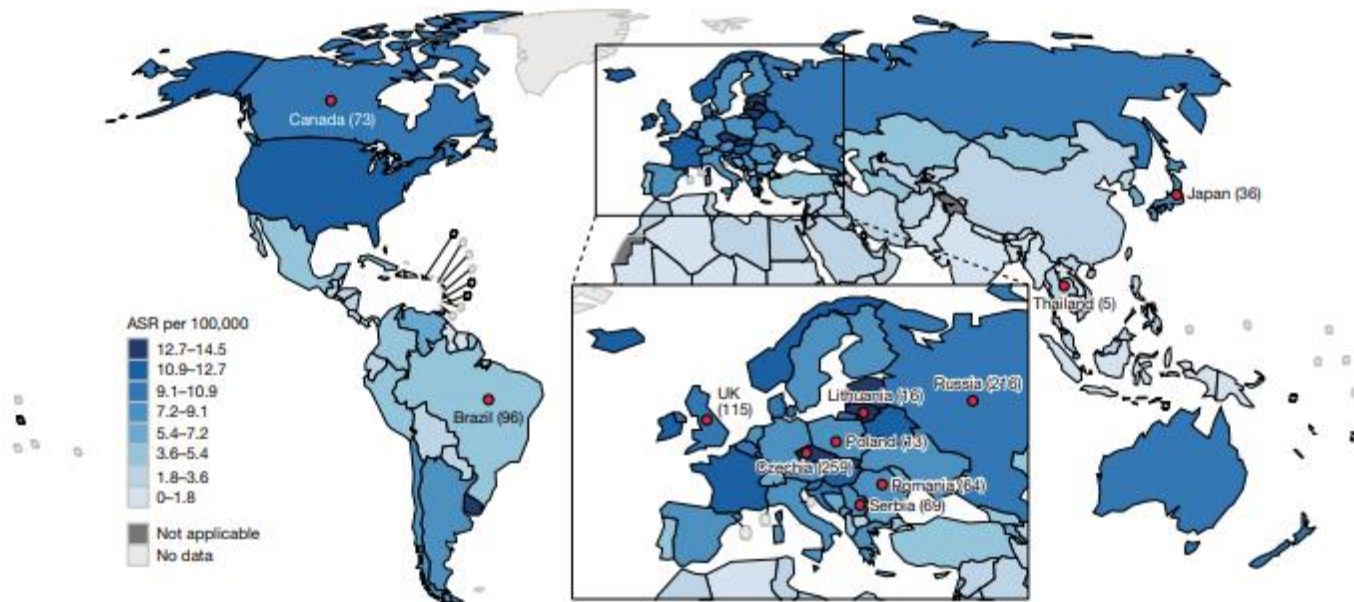
**Figure 2.** The representative mutational signatures, SBS4 and SBS29, are unique enough to be distinguished from others, associated with a specific exposure and are found in the corresponding tumors. SBS4 (top panel) is associated with tobacco use and found primarily in tumors from tobacco smokers (33), while SBS29 (bottom panel) is associated with chewing tobacco and almost exclusively in oral cancers. Both exposures lead to tumors with predominantly C > A mutations; however, the trinucleotide context profile suggests distinct differences in the mutational signatures, and hence perhaps mechanisms, induced by smoking tobacco compared with those induced by chewing tobacco, which could be elucidated by studying of the DNA adductome.



**Figure 3.** Representative mutational signatures, SBS1 and SBS2, are distinct enough to be distinguished from others and are associated with specific endogenous processes. SBS1 (top panel) is thought to result from the spontaneous or enzymatic deamination of 5-Me-Cyt to Thy, while SBS2 (bottom panel) is associated with cytosine deaminase activity, specifically the AID/APOBEC family of cytosine deaminases. Both endogenous processes lead to mutational signatures characterized by C > T mutations; however, each exhibits a unique trinucleotide context profile, suggesting different underlying mechanisms.

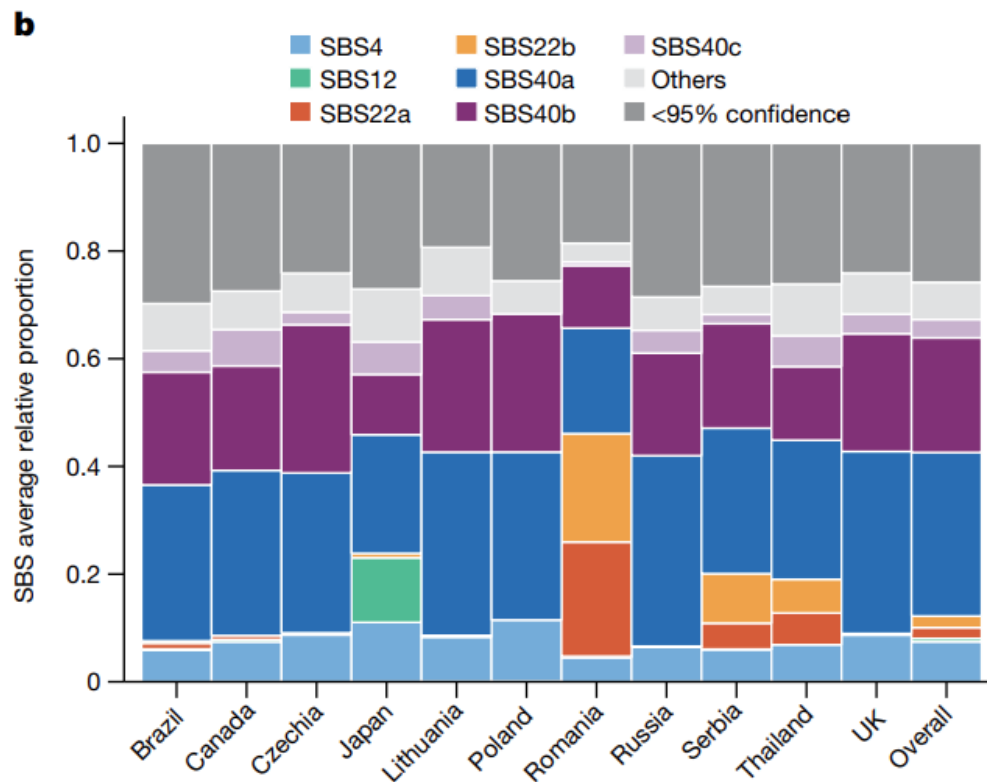


# Geographic variation of mutagenic exposures in kidney cancer genomes (part 1)

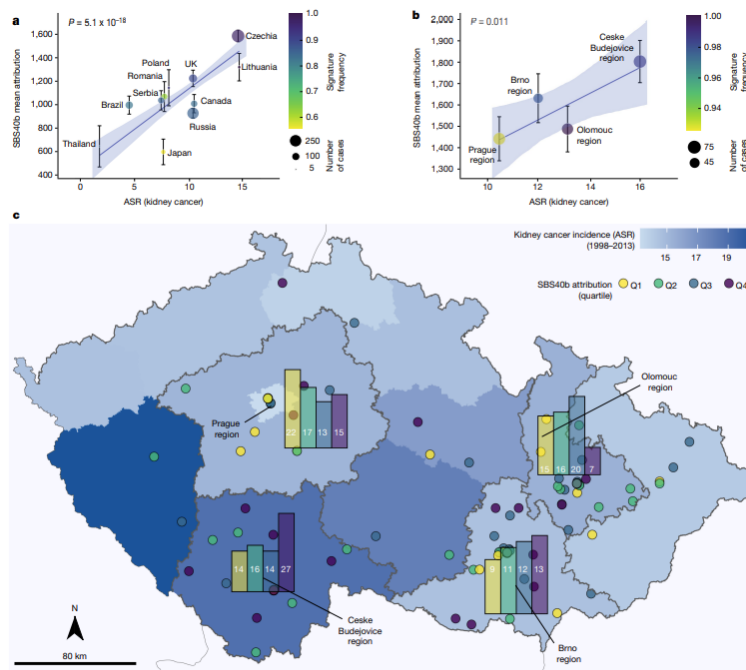


**Fig.1| Eleven participating countries and estimated ASRs of ccRCCs.** Incidence of ccRCC for men and women combined (ASR per 100,000). Data from GLOBOCAN 2020. Markers indicate countries included in this study (number of participants with ccRCC per country).

# Geographic variation of mutagenic exposures in kidney cancer genomes (part 2)



# Geographic variation of mutagenic exposures in kidney cancer genomes (part 3)

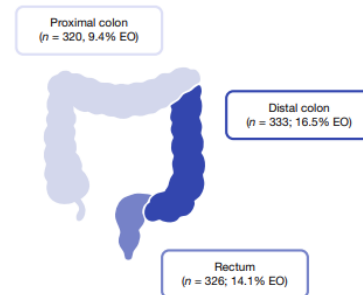
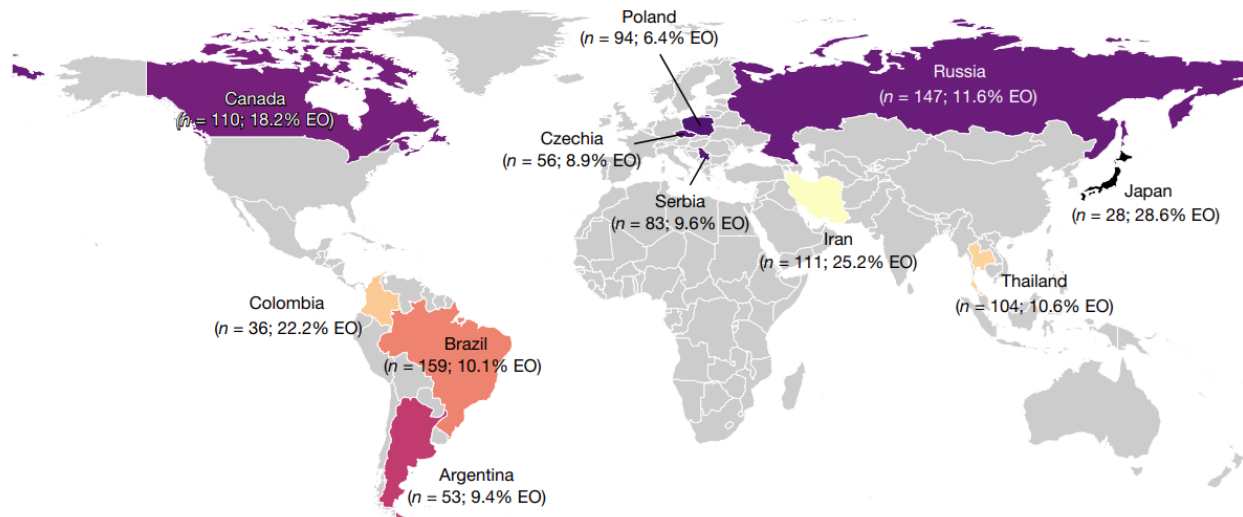
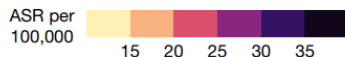


**Fig. 4 | Association of SBS40b signature attribution with incidence of kidney cancer.** **a**, Number of mutations attributed to signature SBS40b against ASR of kidney cancer in each of the 11 countries represented in the cohort. Data are mean  $\pm$  s.e.m. ( $n = 961$  biologically independent samples examined over 1 independent experiment). **b**, Number of mutations attributed to signature SBS40b in four regions of Czech Republic against ASR of kidney

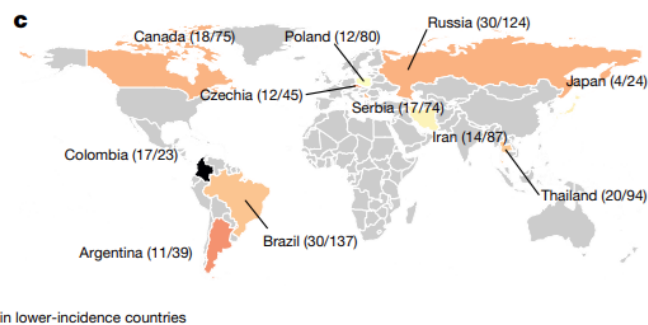
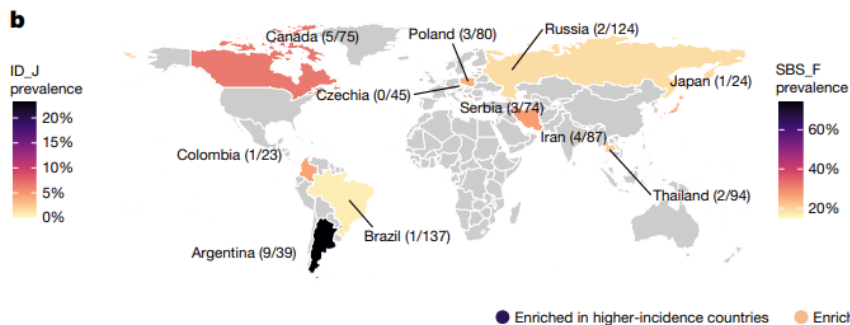
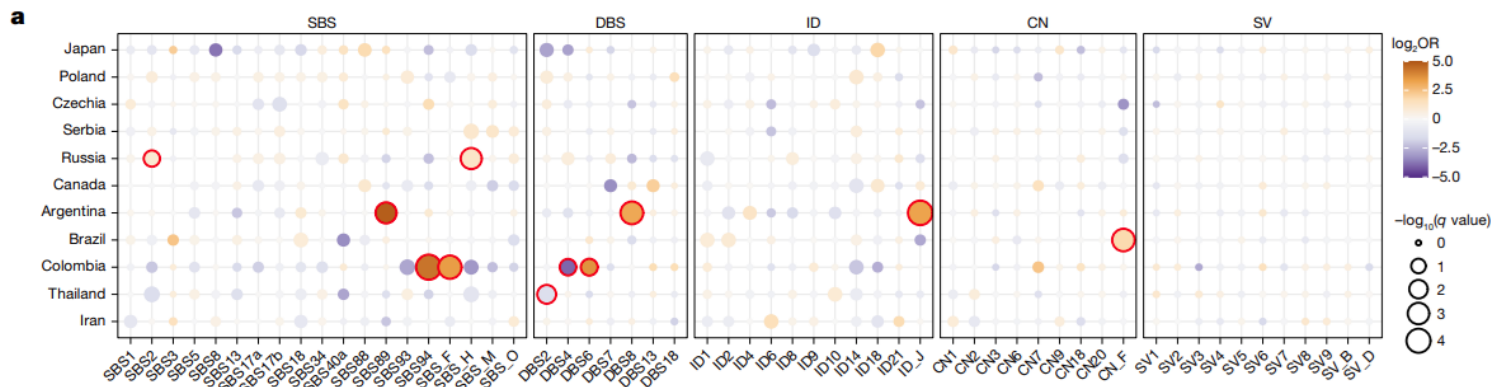
cancer in each region. Data are mean  $\pm$  s.e.m. ( $n = 961$  biologically independent samples examined over 1 independent experiment). **a, b**, P values are shown for the ASR variable in linear regressions across all cases, adjusted for sex and age of diagnosis. **c**, Attribution of SBS40b signature within the Czech Republic, with bar plots showing the number of cases for each quartile of SBS40b attribution across Prague, Olomouc, Ceske Budejovice and Brno regions.

# Geographic and age variations in mutational processes in colorectal cancer (part 1)

a

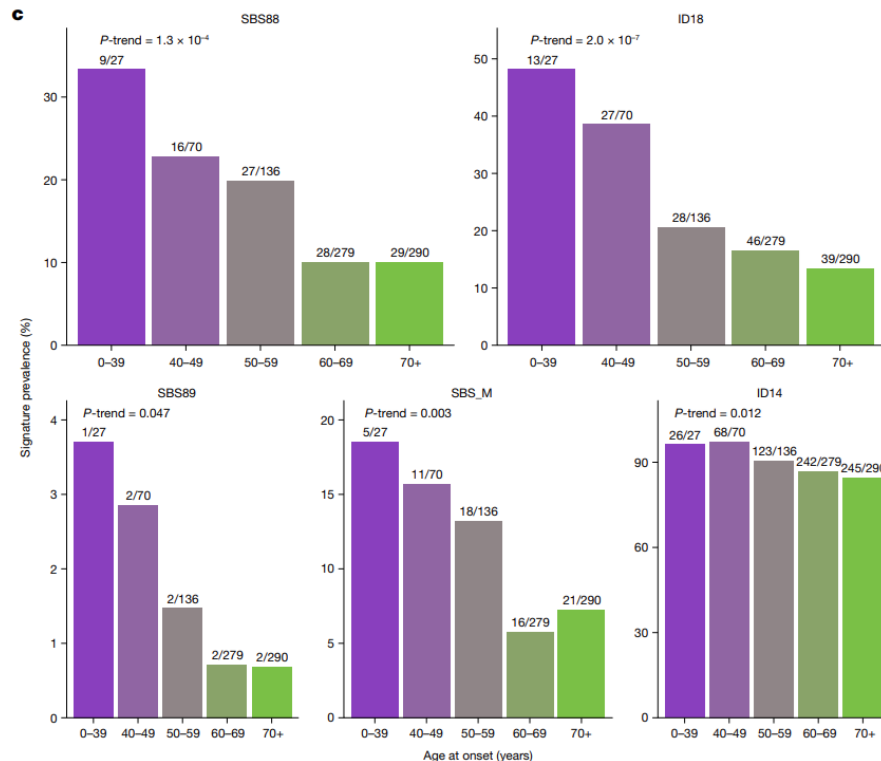


# Geographic and age variations in mutational processes in colorectal cancer (part 2)



● Enriched in higher-incidence countries ● Enriched in lower-incidence countries

# Geographic and age variations in mutational processes in colorectal cancer (part 3)

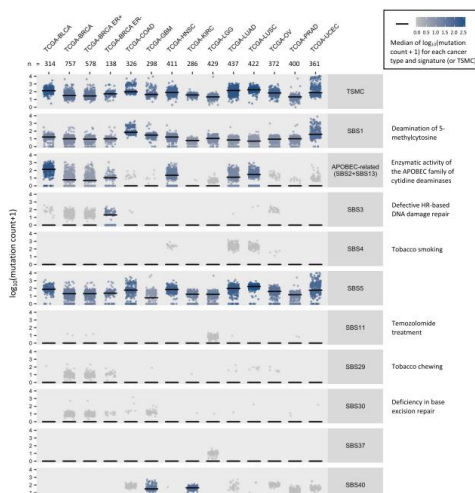




# Somatic mutational profiles and germline polygenic risk scores in human cancer

## Somatic mutational profiles and germline polygenic risk scores in human cancer

Yuxi Liu<sup>1,2</sup>, Alexander Gusev<sup>3</sup>, Yujing J. Heng<sup>4</sup>, Ludmil B. Alexandrov<sup>5</sup> and Peter Kraft<sup>1,2,6\*</sup>



**Fig. 1** Mutation counts of SBS signatures and TSMC across 12 TCGA cancer types and two subtypes of breast cancer. Each dot represents a tumor sample. The median of  $\log_2(\text{mutation count} + 1)$  for each cancer type (or subtype) and SBS signature (or TSMC) is represented by both the color of the dots and the short black line in each panel. The number of TCGA samples for each cancer type is shown on the top.

**Table 1** Significant associations between tumor somatic mutation counts and germline PRS

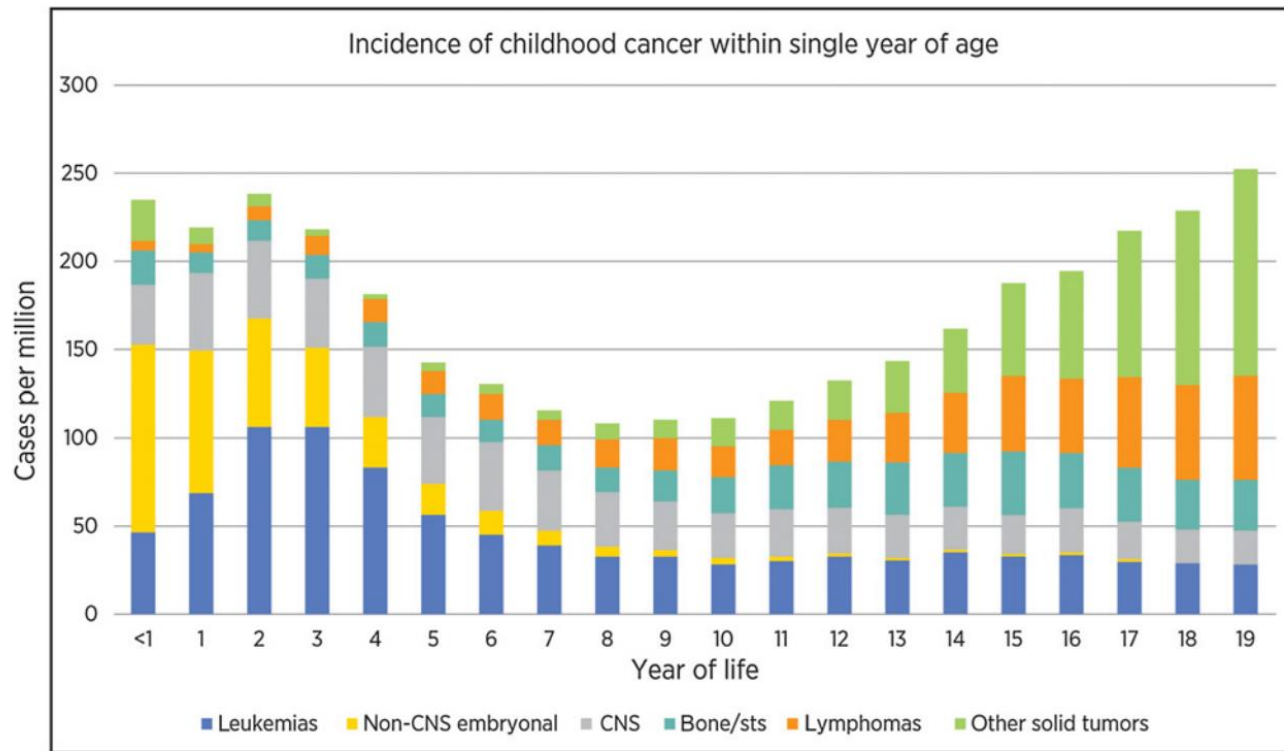
Cancer type	Somatic mutation count	Germline PRS <sup>a</sup>	Direction of association <sup>b</sup>	p value <sup>c</sup>
PRAD	SBS1	Age at menarche	—	$2.49 \times 10^{-9}$
PRAD	SBS1	IBD	+	$9.04 \times 10^{-6}$
PRAD	SBS1	CD	+	$4.63 \times 10^{-8}$
PRAD	SBS1	UC	+	$3.71 \times 10^{-9}$
PRAD	SBS1	GBM	—	$3.29 \times 10^{-8}$
PRAD	SBS1	HNSC	—	$2.07 \times 10^{-9}$
PRAD	SBS1	BMI	+	$6.09 \times 10^{-8}$
PRAD	SBS1	Drinks per week	—	$1.69 \times 10^{-5}$
BRCA	APOBEC-related <sup>d</sup>	IBD	+	$1.79 \times 10^{-6}$
BRCA	SBS1	Age at menarche	+	$1.47 \times 10^{-5}$
BRCA ER+	SBS1	Age at menarche	+	$2.89 \times 10^{-5}$
BRCA ER-	SBS1	HNSC	—	$1.99 \times 10^{-6}$
BRCA ER-	TSMC	HNSC	—	$5.31 \times 10^{-7}$
COAD	SBS1	Cigarettes per day	—	$1.71 \times 10^{-5}$
COAD	TSMC	HNSC	—	$1.71 \times 10^{-5}$
GBM	SBS1	OV	+	$1.97 \times 10^{-5}$
UCEC	SBS40	CD	—	$7.71 \times 10^{-7}$

<sup>a</sup> PRS is calculated from the germline genetic data of the same TCGA patient as the tumor sample

<sup>b</sup> Direction of the association between somatic mutation count and PRS from zero-inflated negative binomial model, negative binomial model, or linear model adjusting for age at cancer diagnosis, sex, and the top 10 genetic PCs

<sup>c</sup> P value associated with PRS. P values are obtained from likelihood ratio test of model with PRS and model without PRS. For zero-inflated negative binomial model, the results are from testing the count and logistic model jointly. Age at cancer diagnosis, sex, and the top 10 genetic PCs were adjusted as covariates in all models

<sup>d</sup> APOBEC-related signature count is the sum of SBS2 and SBS13 mutation counts, both signatures are attributed to the enzymatic activity of the APOBEC family of cytidine deaminases



**Figure 2.**  
Distribution of tumors across the pediatric age spectrum.

Spector and Lupo, 2020

# Sex Ratio Among Childhood Cancers by Single Year of Age

## Sex ratio among childhood cancers by single year of age

Lindsay A. Williams<sup>1</sup>  | Michaela Richardson<sup>1</sup> | Erin L. Marcotte<sup>1,2</sup>

Jenny N. Poynter<sup>1,2</sup> | Logan G. Spector<sup>1,2</sup>

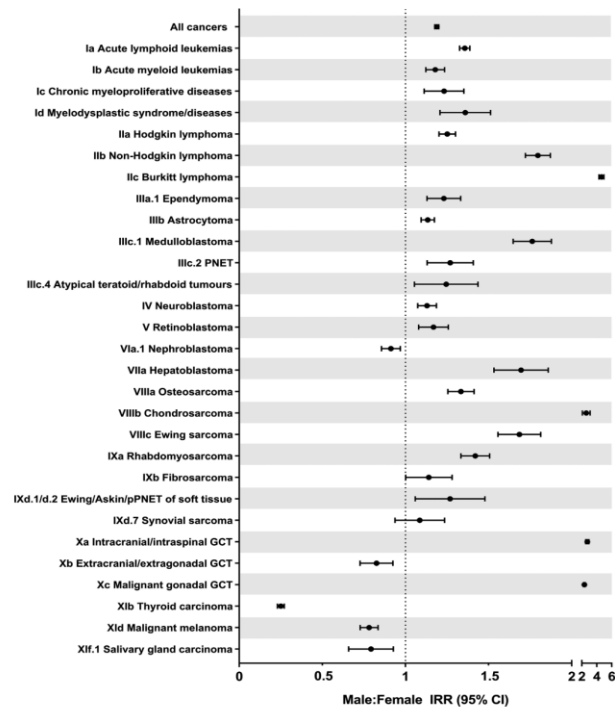
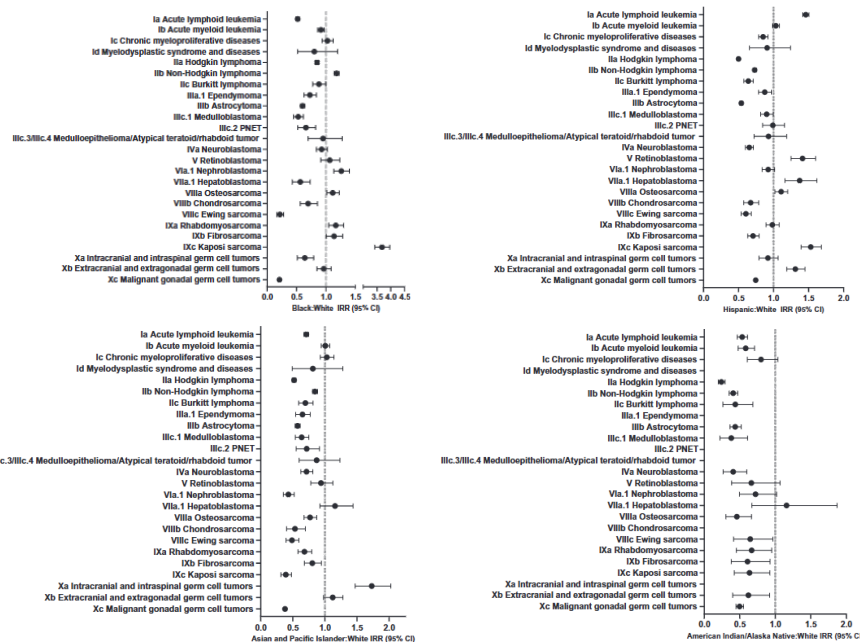


FIGURE 1 Male-to-female incidence rate ratios (IRR) and corresponding 95% confidence intervals for childhood cancer by tumor type (ICCC designation) for all ages combined, SEER 18 (2000–2015)

# Racial and ethnic disparities in pediatric cancer incidence among children and young adults in the United States by single year of age

## Racial and Ethnic Disparities in Pediatric Cancer Incidence Among Children and Young Adults in the United States by Single Year of Age

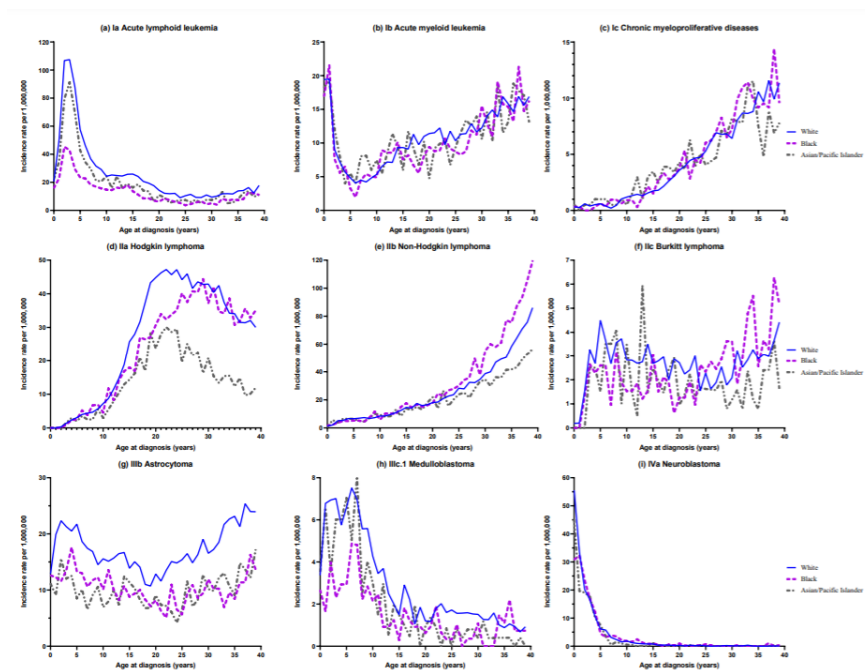
Erin L. Marcotte, PhD <sup>1,2</sup>, Allison M. Domingues, MS<sup>1</sup>, Jeannette M. Sample, MPH <sup>1,2</sup>, Michaela R. Richardson, MPH<sup>1</sup>, and Logan G. Spector, PhD<sup>1,2</sup>



# Racial and ethnic disparities in pediatric cancer incidence among children and young adults in the United States by single year of age

## Racial and Ethnic Disparities in Pediatric Cancer Incidence Among Children and Young Adults in the United States by Single Year of Age

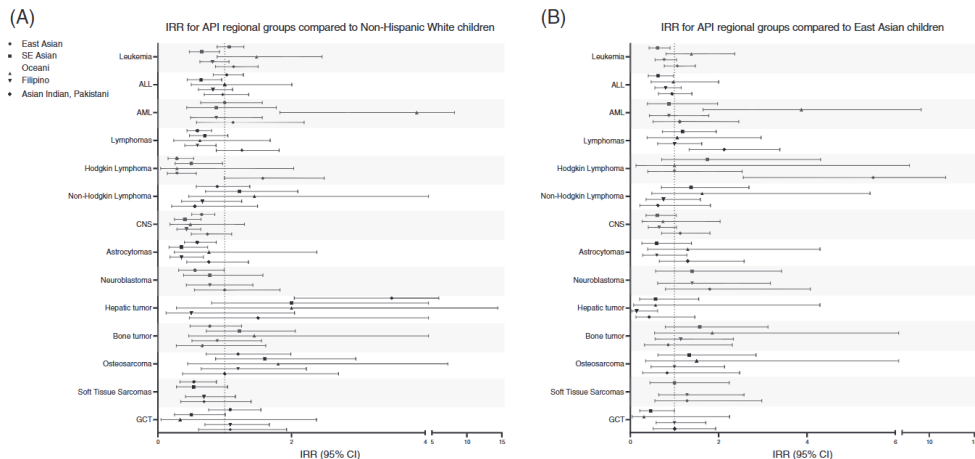
Erin L. Marcotte, PhD <sup>1,2</sup>, Allison M. Domingues, MS<sup>1</sup>, Jeannette M. Sample, MPH <sup>1,2</sup>, Michaela R. Richardson, MPH<sup>1</sup>, and Logan G. Spector, PhD<sup>1,2</sup>



# Childhood cancer incidence among specific Asian and Pacific Islander populations in the United States

## Childhood cancer incidence among specific Asian and Pacific Islander populations in the United States

Kristin J. Moore<sup>1</sup> | Aubrey K. Hubbard<sup>2</sup> | Lindsay A. Williams<sup>2,3</sup> | Logan G. Spector<sup>2,3</sup>

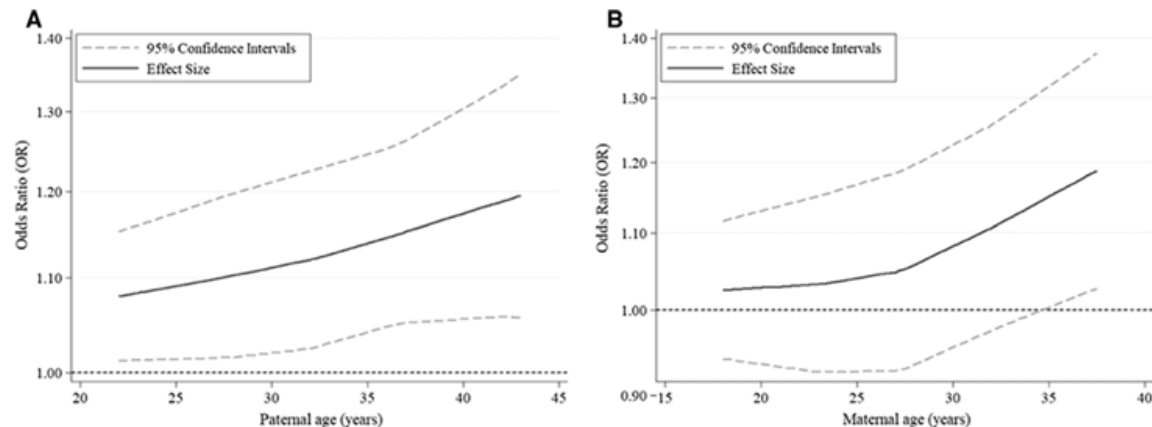


**FIGURE 1** Incidence rate ratios (IRR) and 95% confidence intervals (CI) for US-based Asian and Pacific Islander (API) regional groups compared to, A, Non-Hispanic White children and B, East Asian children, SEER Detailed Asian/Pacific Islander Database<sup>10</sup> (1998-2002; Low Population) and SEER 13<sup>11</sup> (1998-2002)

# Advanced parental age as a risk factor for childhood acute lymphoblastic leukemia: results from studies of the Childhood Leukemia International Consortium

## Advanced parental age as risk factor for childhood acute lymphoblastic leukemia: results from studies of the Childhood Leukemia International Consortium

Eleni Th. Petridou<sup>1,2</sup> · Marios K. Georgakis<sup>1</sup> · Friederike Erdmann<sup>3,4</sup> · Xiaomei Ma<sup>5</sup> · Julia E. Heck<sup>6</sup> · Anssi Auvinen<sup>7</sup> · Beth A. Mueller<sup>8,9</sup> · Logan G. Spector<sup>10</sup> · Eve Roman<sup>11</sup> · Catherine Metayer<sup>12</sup> · Corrado Maria S. Pombo-de-Oliveira<sup>14</sup> · Sameera Ezzat<sup>15</sup> · Michael E. Scheurer<sup>16</sup> · Ana Maria Mora<sup>17</sup> · John D. Johnni Hansen<sup>19</sup> · Alice Y. Kang<sup>12</sup> · Rong Wang<sup>9</sup> · David R. Doody<sup>8</sup> · Eleanor Kane<sup>11</sup> · Waffa M. Rash Nick Dessypris<sup>1</sup> · Joachim Schüz<sup>2</sup> · Claire Infante-Rivard<sup>22</sup> · Alkistis Skalkidou<sup>23</sup>

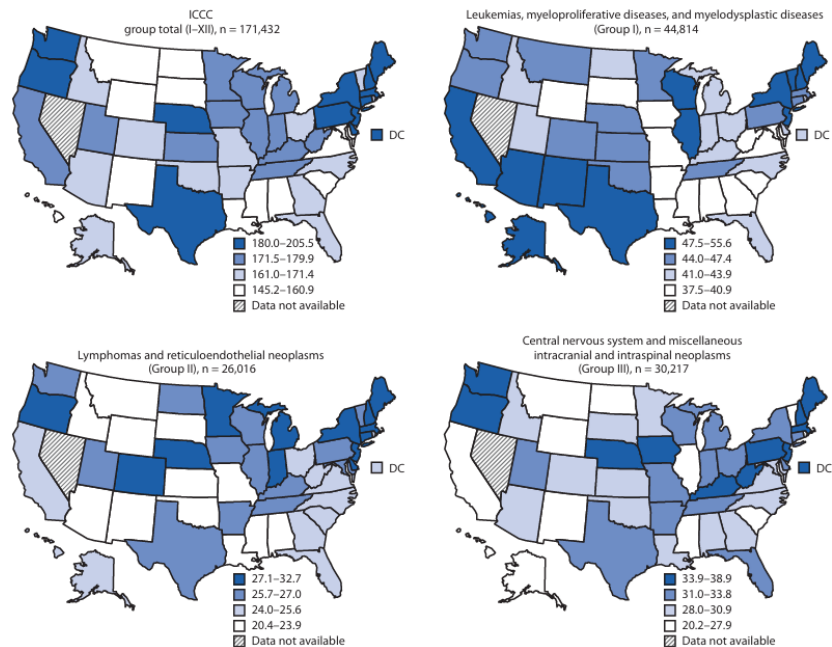


**Fig. 2** Curves depicting the association of (A) paternal and (B) maternal age with childhood (0–14 years) acute lymphoblastic leukemia, as derived from meta-analysis restricted cubic spline models encompassing the five registry-based case-control studies (Canada-Quebec;

Denmark; Finland; US, California State, CCLRP; US, Washington State). The solid line depicts the effect estimate (Odds Ratio), whereas dash-lines correspond to 95% confidence intervals

# Geographic variation in pediatric cancer incidence — United States, 2003-2014

David A. Siegel, MD<sup>1,2</sup>; Jun Li, MD, PhD<sup>2</sup>; S. Jane Henley, MSPH<sup>2</sup>; Reda J. Wilson, MPH<sup>2</sup>; Natasha Buchanan Lunsford, PhD<sup>2</sup>; Eric Tai, MD<sup>2</sup>; Elizabeth A. Van Dyne, MD<sup>1,2</sup>





**Table 1.** Confirmed and suspected risk factors for selected childhood cancers.

	ALL	AML	NB	HB	RB	WT	MB	PNET	Ependymoma	Astrocytoma	Strength of evidence
<b>Preconception/pregnancy</b>											
Smoking											++
Vitamins											++
Occupational exposures											++
Residential exposures											++
Coffee											+
Alcohol											++
Ionizing radiation											+++
<b>Birth</b>											
Maternal age											++
Paternal age											++
Chromosomal birth defects											+++
Non-chromosomal birth defects											+++
High birth weight											+++
Low birth weight											+++
C-section											+
Gestational age											+
<b>Childhood</b>											
Breastfeeding											+
Allergies											++
Residential chemical											+
Passive smoke											+
Irradiation											++

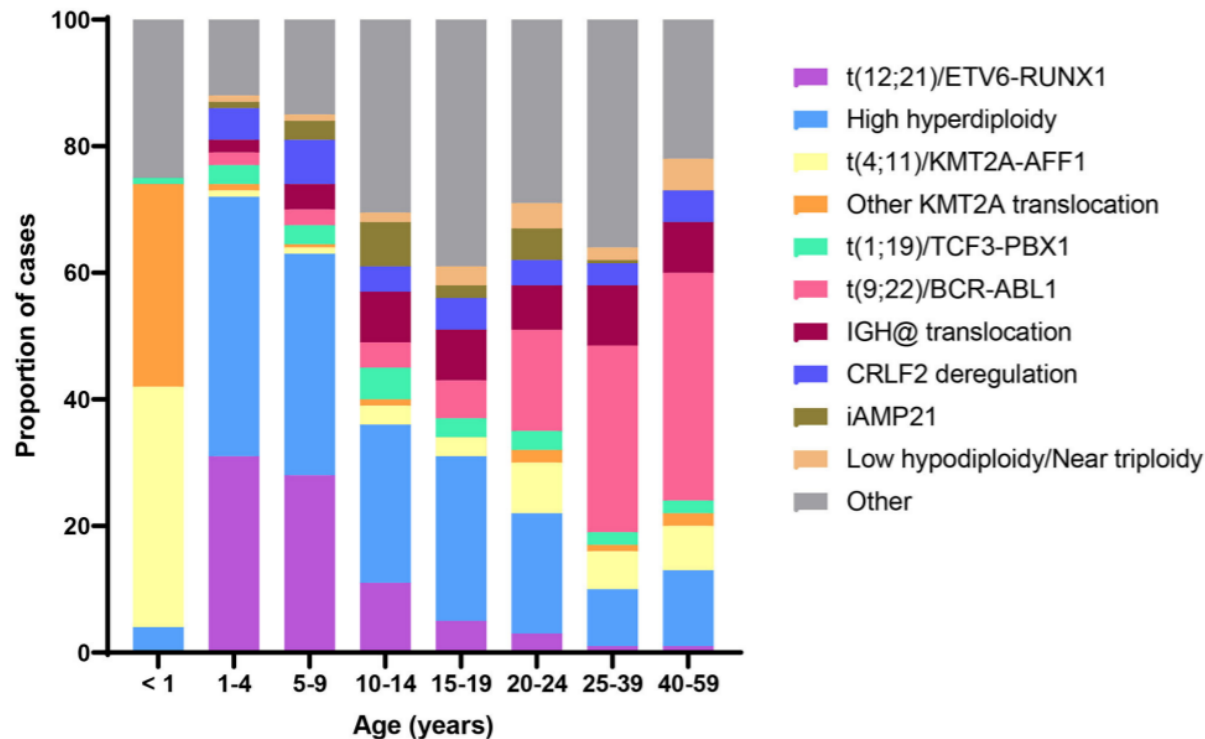
Note: Taken from refs. 25, 30, 31,103-266. For strength of evidence: + epidemiologic evidence with little mechanistic support; ++ can cross placenta or has developmental consequences but epidemiologic evidence is equivocal; +++ strong epidemiologic and mechanistic evidence.

Abbreviations: ALL, acute lymphoblastic leukemia; AML, acute myeloid leukemia; HB, hepatoblastoma; MB, medulloblastoma; NB, neuroblastoma; PNET, primitive neuroectodermal tumor; RB, retinoblastoma; WT, Wilms tumor.

**Legend**

Positive, effect estimate <1.5	
Positive, effect estimate ≥1.5	
No association	
Negative, effect estimate >0.67	
Negative, effect estimate ≤0.67	
Inconclusive	

Spector and Lupo, 2020



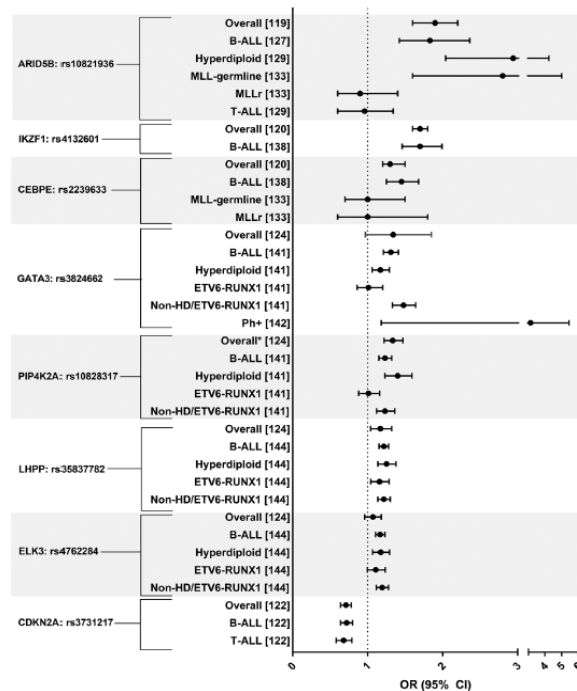
**FIGURE 2 |** Distribution of B-cell acute lymphoblastic leukemia (ALL) cytogenetic subtypes by age at diagnosis. Data adapted from (6).

Marcotte, Spector, Mendes-de-Almeida, and Nelson, 2021

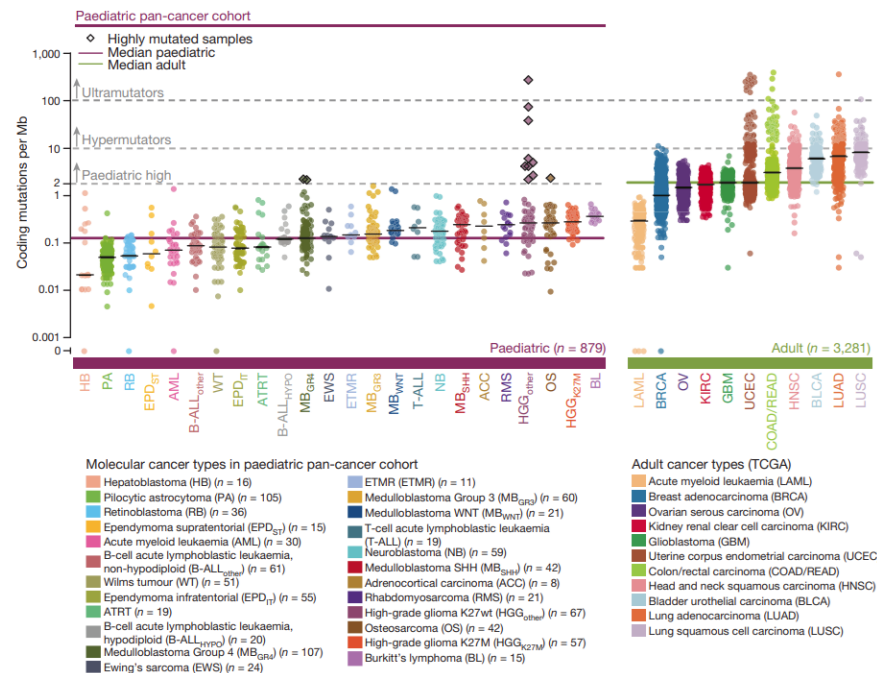
# Is there etiologic heterogeneity between subtypes of childhood acute lymphoblastic leukemia? A review of variation in risk by subtype

## Is There Etiologic Heterogeneity between Subtypes of Childhood Acute Lymphoblastic Leukemia? A Review of Variation in Risk by Subtype

Lindsay A. Williams<sup>1</sup>, Jun J. Yang<sup>2,3</sup>, Betsy A. Hirsch<sup>4,5</sup>, Erin L. Marcotte<sup>1,5</sup>, and Logan G. Spector<sup>1,5</sup>



# The landscape of genomic alterations across childhood cancers



**Figure 1 | Somatic mutations in the paediatric pan-cancer cohort.** Somatic coding mutation frequencies in 24 paediatric ( $n = 879$ ) primary tumours) and 11 adult ( $n = 3,281$ ) cancer types (TCGA)<sup>7</sup>. Hypermutated

and highly mutated samples are separated by dashed grey lines and highlighted with black squares. Median mutation loads are shown as solid lines (black, cancer types; purple, all paediatric; green, all adult).

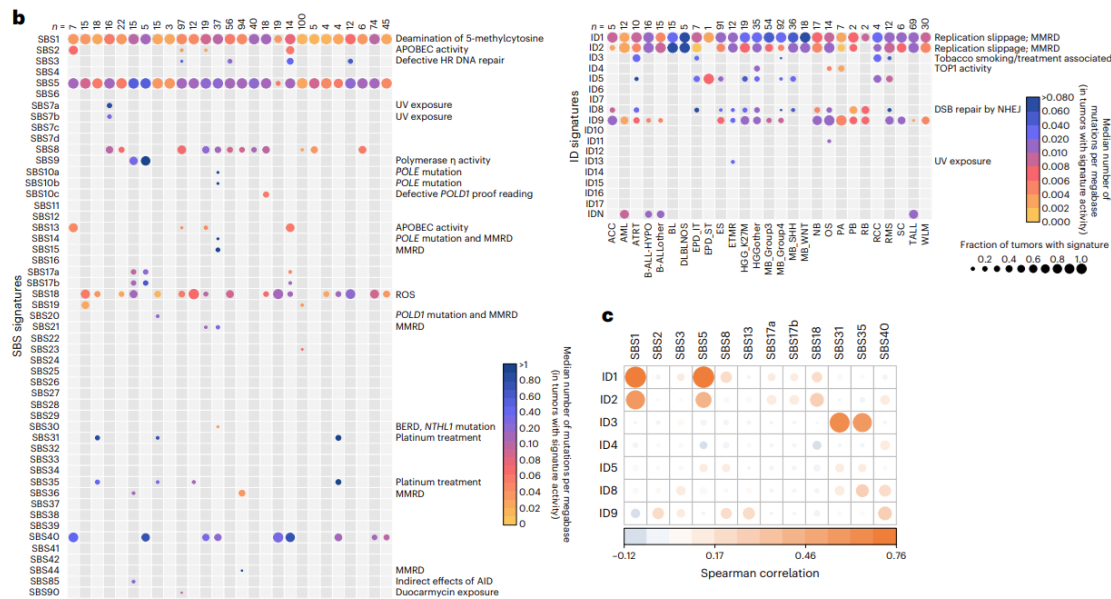
# Comprehensive analysis of mutational signatures reveals distinct patterns and molecular processes across 27 pediatric cancers (part 1)



**Figure 1 | Somatic mutations in the paediatric pan-cancer cohort.** Somatic coding mutation frequencies in 24 paediatric ( $n = 879$ ) primary tumours and 11 adult ( $n = 3,281$ ) cancer types (TCGA)<sup>7</sup>. Hypermutated

and highly mutated samples are separated by dashed grey lines and highlighted with black squares. Median mutation loads are shown as solid lines (black, cancer types; purple, all paediatric; green, all adult).

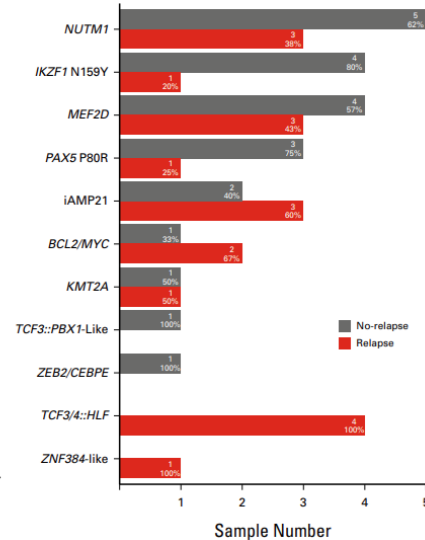
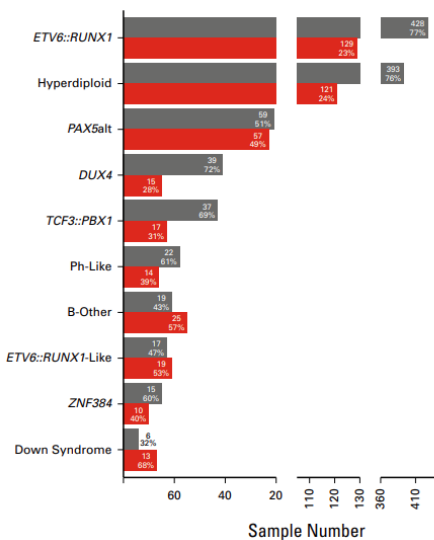
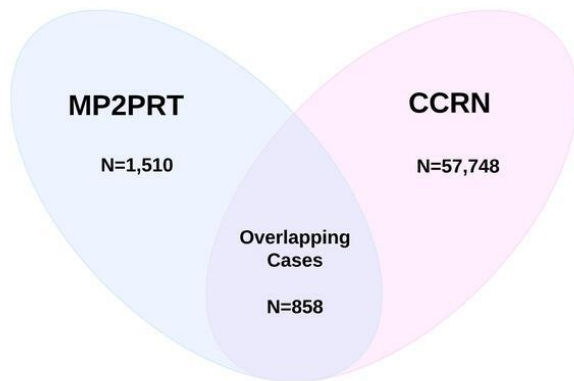
# Comprehensive analysis of mutational signatures reveals distinct patterns and molecular processes across 27 pediatric cancers (part 2)



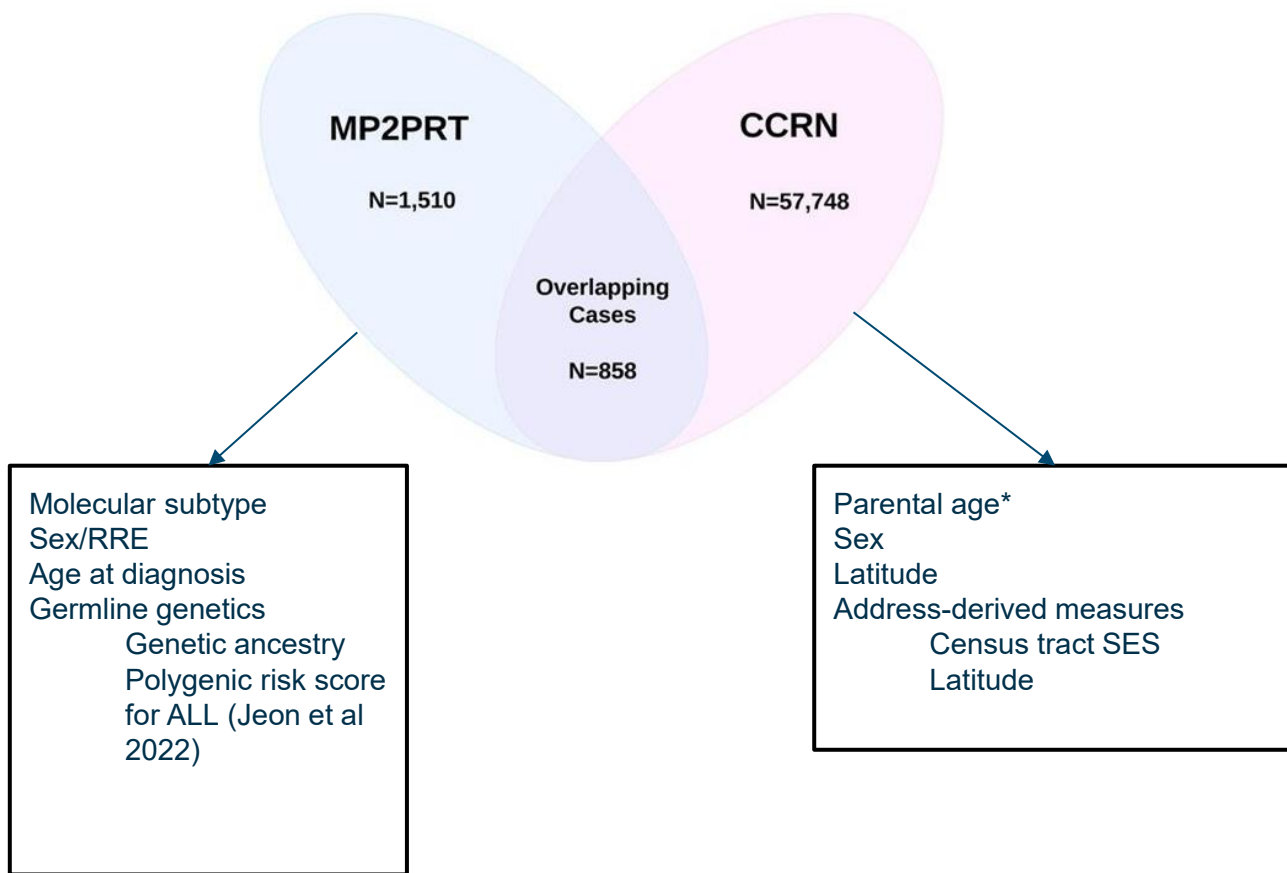
# PEDIATRIC MUTOGRAPH



# Molecular Profiling to Predict Response to Treatment (MP2PRT)



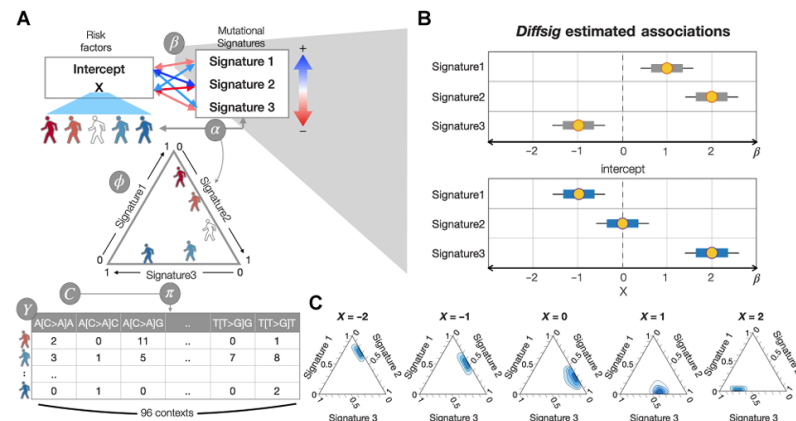




# Diffsig: Associating Risk Factors with Mutational Signatures

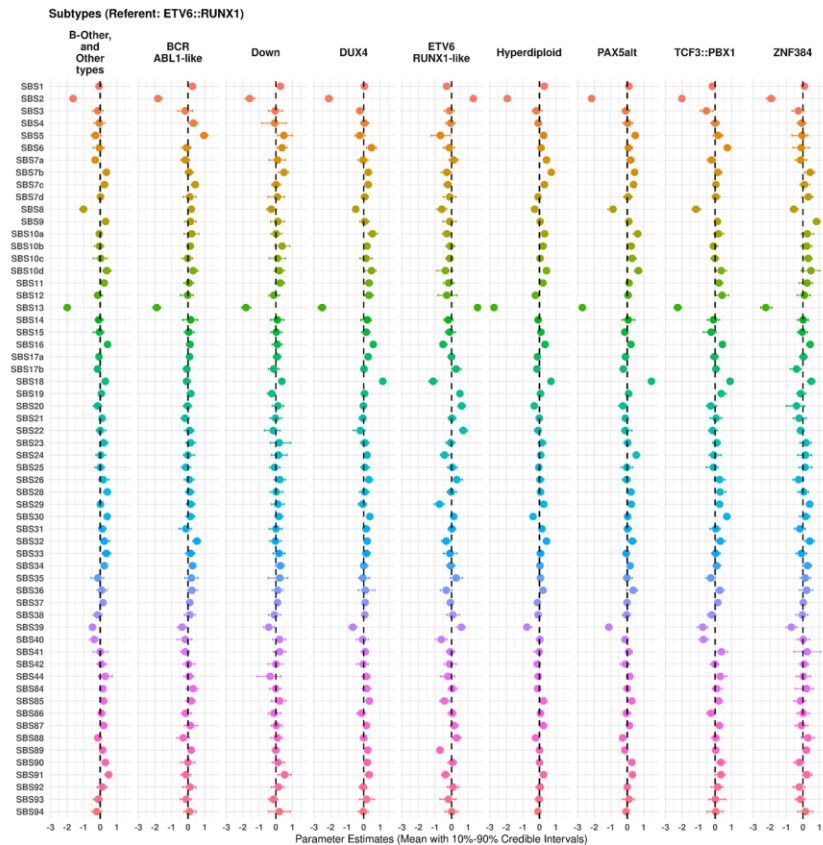
## Diffsig: Associating Risk Factors with Mutational Signatures

Ji-Eun Park<sup>1</sup>, Markia A. Smith<sup>2</sup>, Sarah C. Van Alsten<sup>3</sup>, Andrea Walens<sup>3</sup>, Di Wu<sup>1,4</sup>, Katherine A. Hoadley<sup>5,6</sup>, Melissa A. Troester<sup>2,3,5</sup>, and Michael I. Love<sup>1,6</sup>

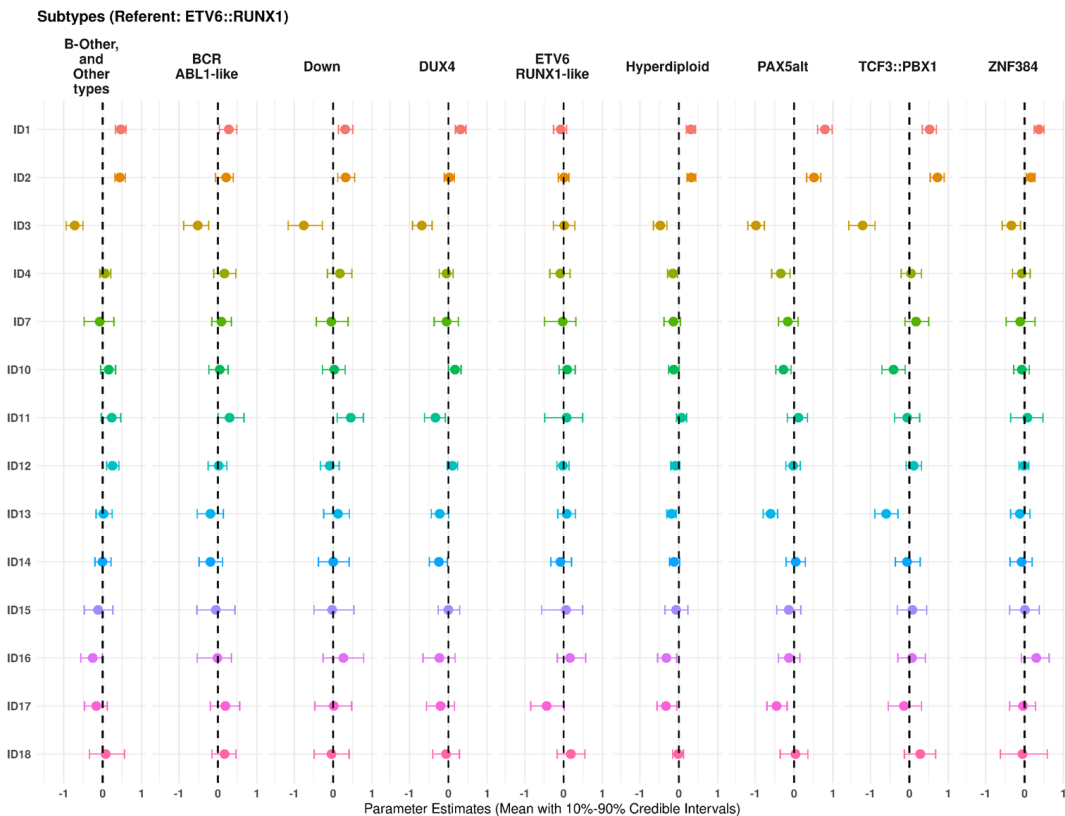


**Figure 1.** Schematic of Diffsig model. **A**, Conceptual diagram of Diffsig, for detecting associations between risk factors and mutational signatures (with these target parameters defined as  $\beta$ ). Each sample's observed somatic mutations are composed of the association ( $\beta$ ) and the sample's risk factor traits (X). Associations between samples and signatures are defined as  $\alpha$ . Even for samples with the same risk factor values, there exists variance among their signature distribution; here, the center of a distribution per sample is diagrammed. The signature contribution is then multiplied by known transition probabilities for a set of reference signatures (C). Finally the resulting mutation probability  $\pi$  underlies the observed mutation counts (Y). **B**, Diffsig estimates the associations  $\beta$  (yellow dots, point estimates; colored bars, 80% CI; and black lines, 95% CIs) for the left example. **C**,  $\beta$ 's effect on  $\pi$  across a range of values of X.  $\beta$  can be interpreted by the strength and direction in which the central tendency of  $\pi$  moves across the space between signatures with differing values of X. From the ternary plots, we can see that as the X increases, the contribution of signature 1 and 2 decreases and that of signature 3 increases. Signature 1 contribution decreases more drastically than signature 2, indicating a negative association of signature 1 and positive values of X.

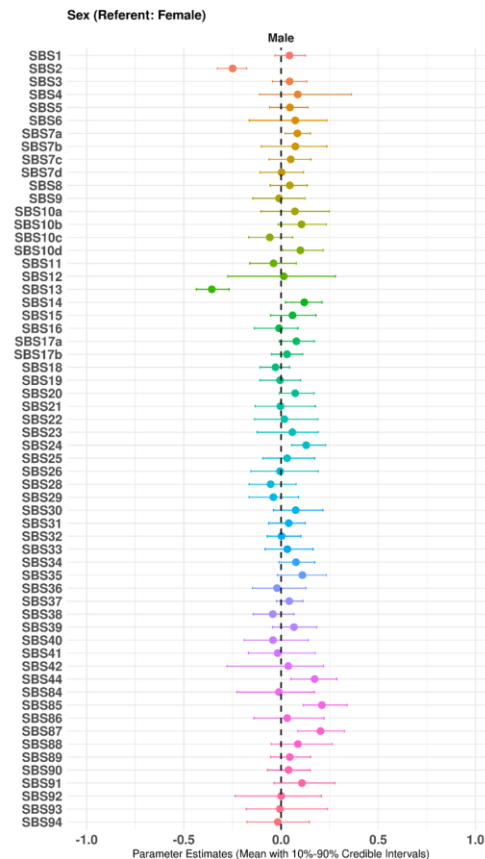
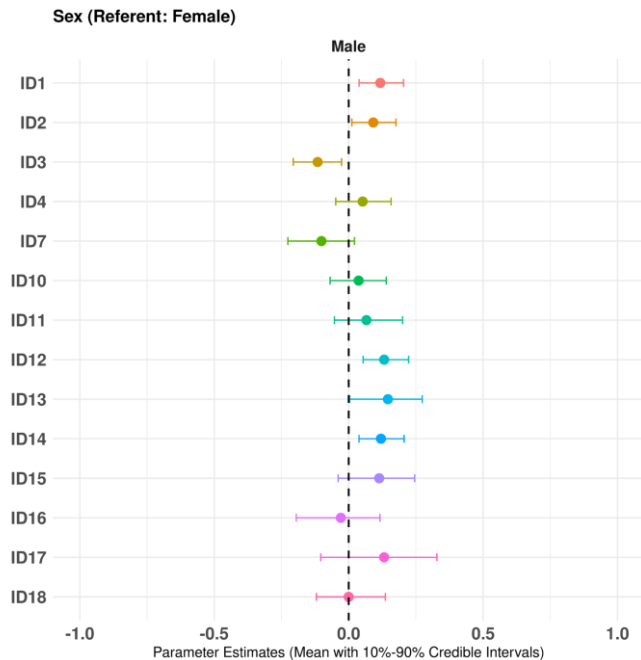
# MP2PRT (n = 1510): Molecular Subtype (Part 1)



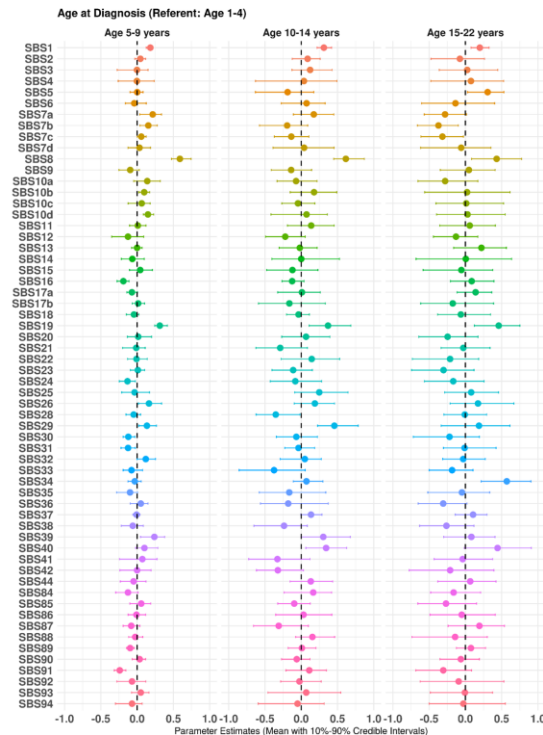
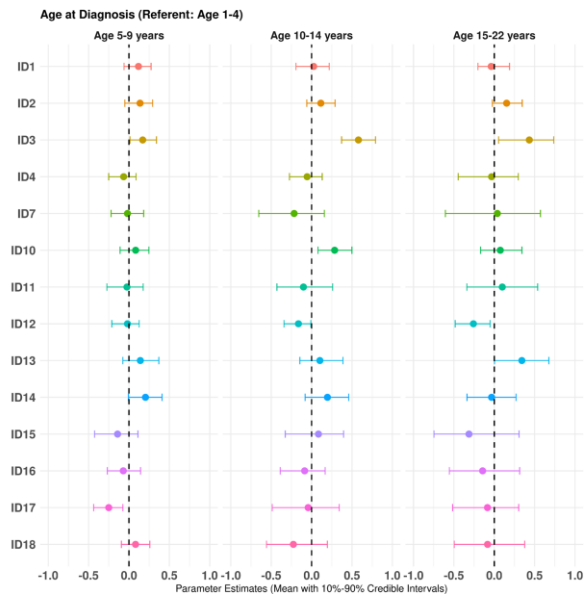
# MP2PRT (n = 1510): Molecular Subtype (Part 2)



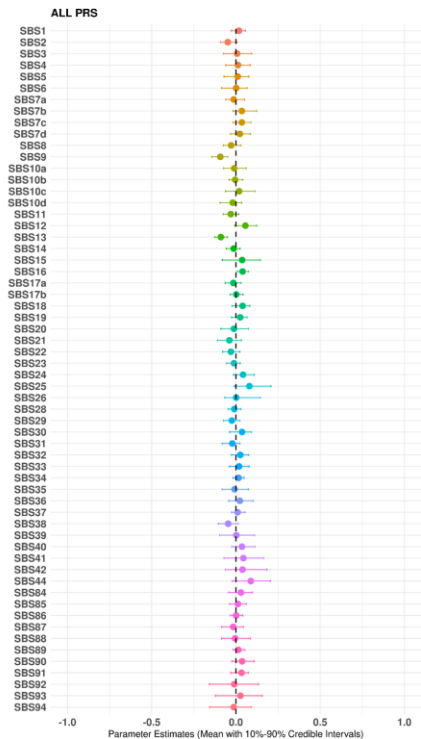
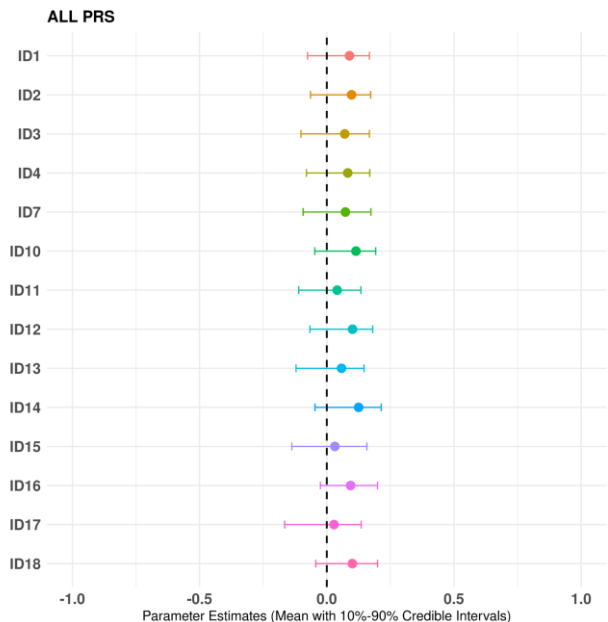
# MP2PRT (n = 1510): Sex



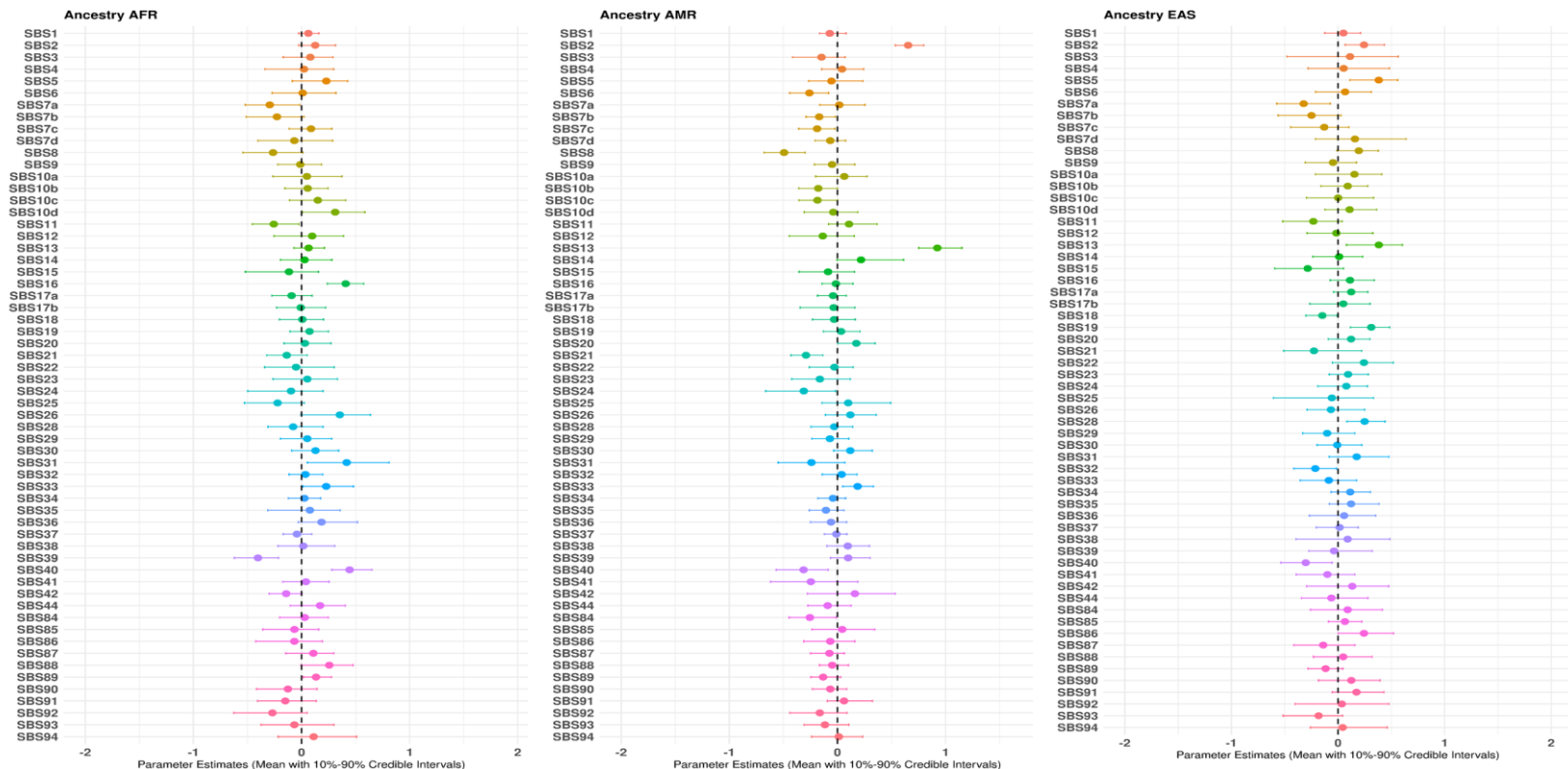
# MP2PRT (n = 1510): Age at Diagnosis



# MP2PRT (n = 1510): ALL Polygenic Risk Score

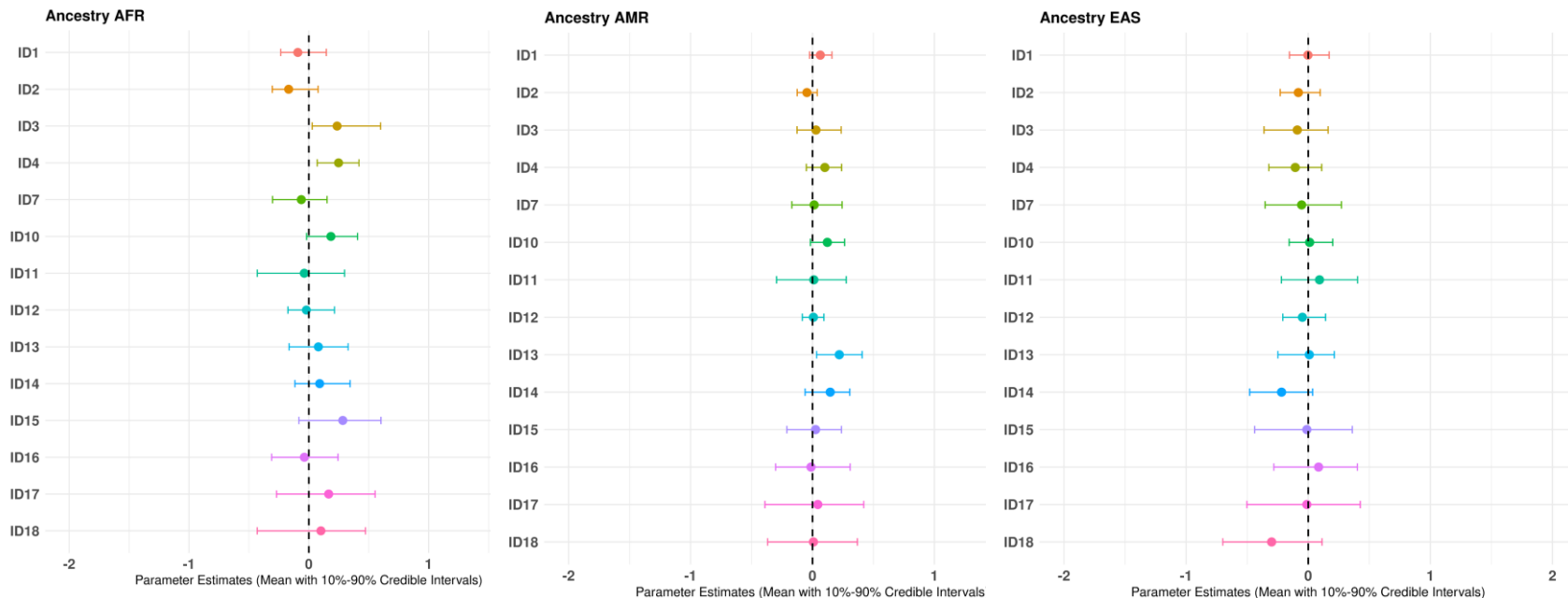


# MP2PRT (n = 1510): Genetic Ancestry (Part 1)

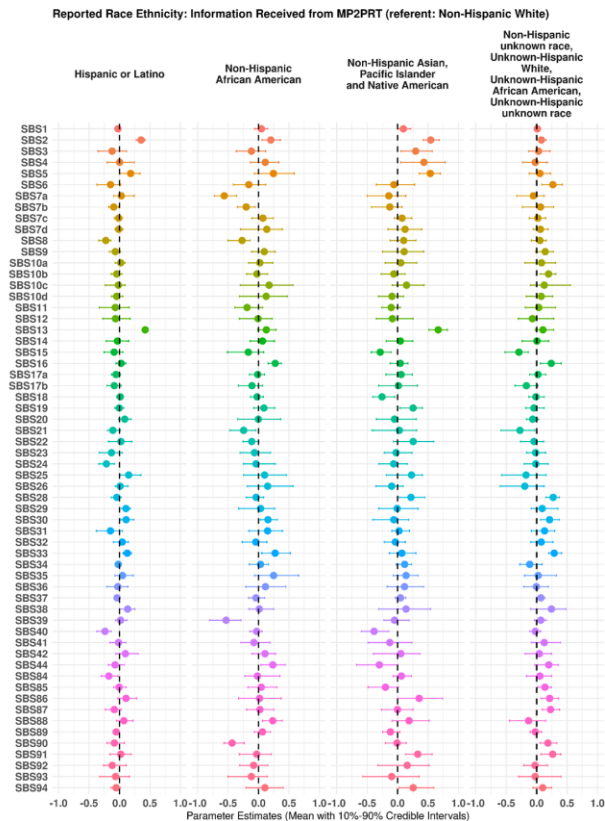




# MP2PRT (n = 1510): Genetic Ancestry (Part 2)

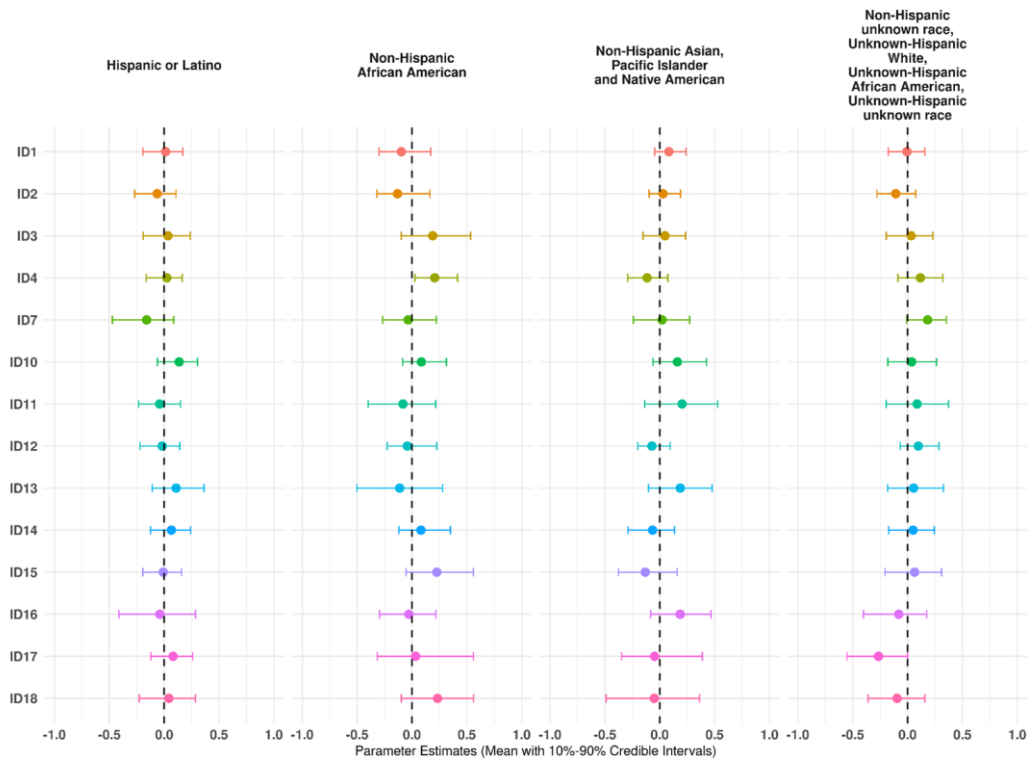


# MP2PRT (n = 1510): Reported Race/Ethnicity (Part 1)

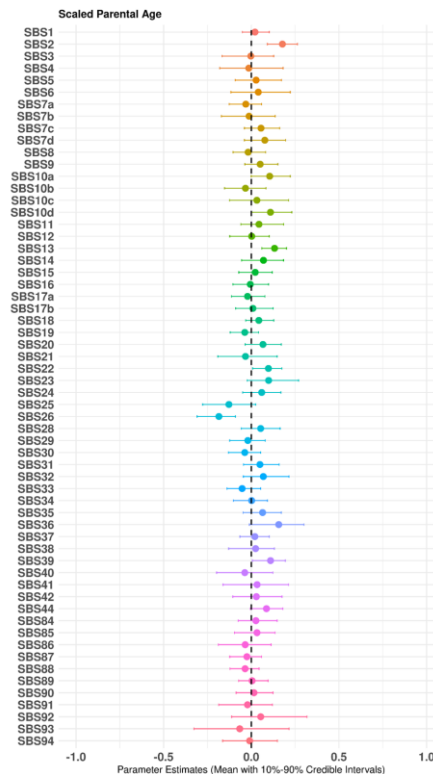
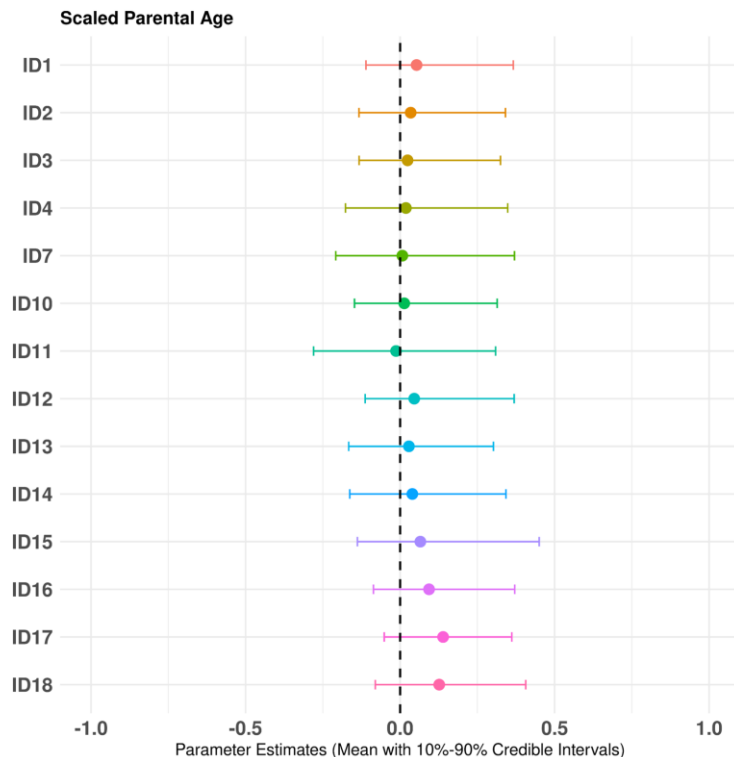


# MP2PRT (n = 1510): Reported Race/Ethnicity (Part 2)

Reported Race Ethnicity: Information Received from Overlapping (Referent:Non-Hispanic White)

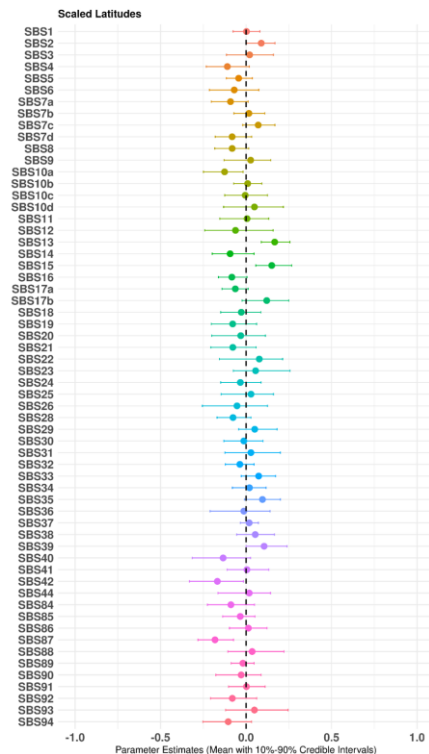
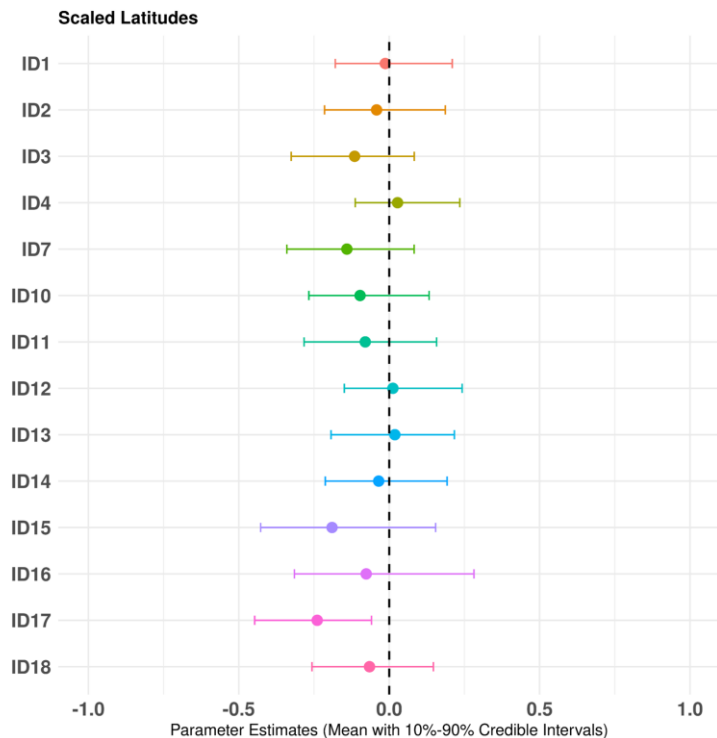


### MP2PRT/CCRN (n = 858): Parental Age\*

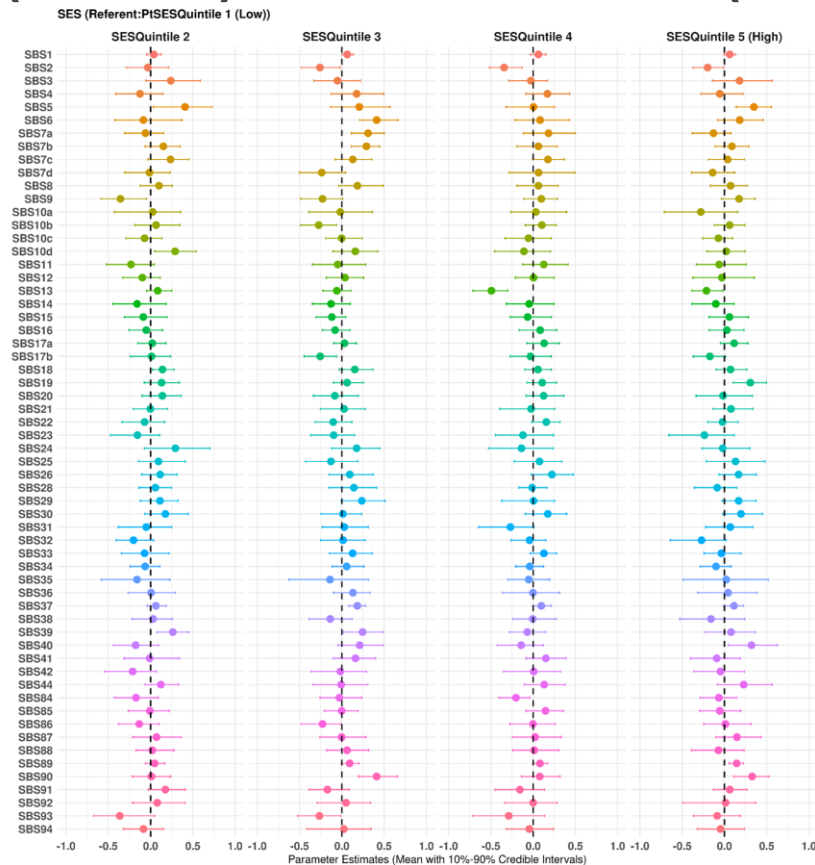


\*Greater of parent/guardian 1 or parent/guardian2 age in CCRN data

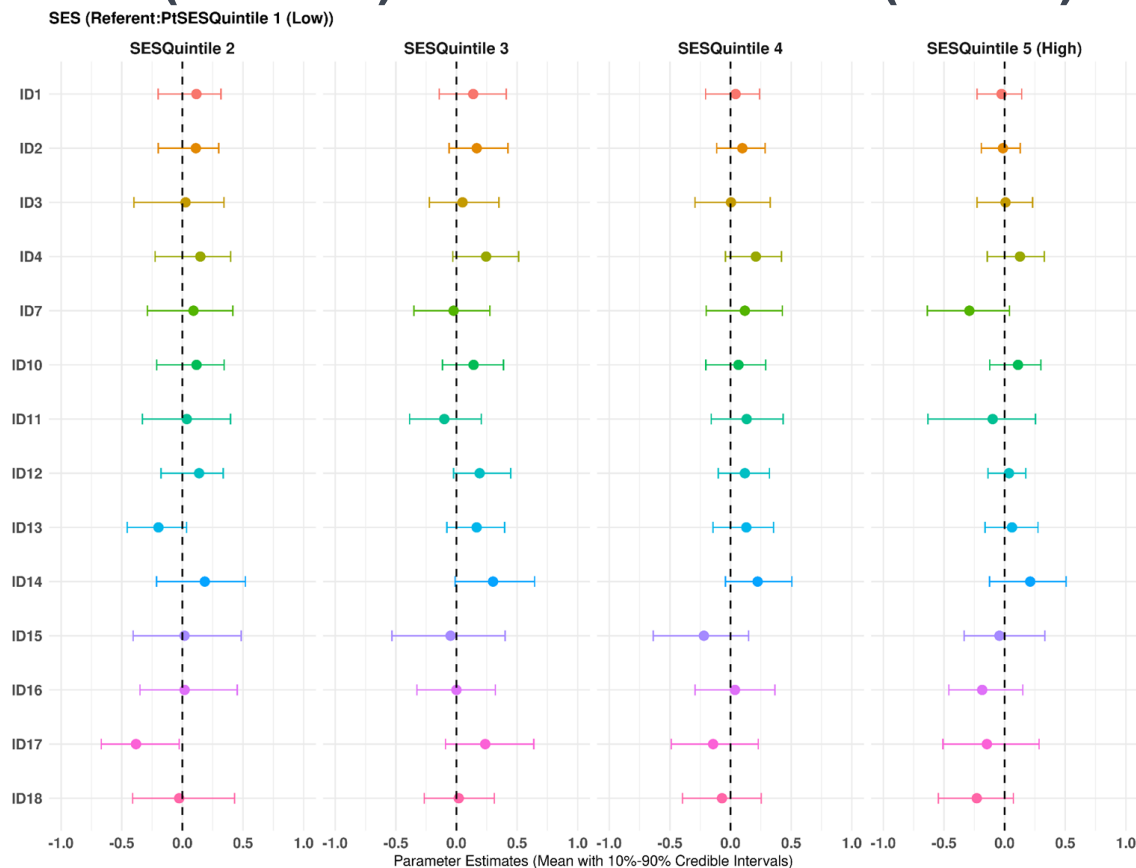
# MP2PRT/CCRN (n = 858): Latitude



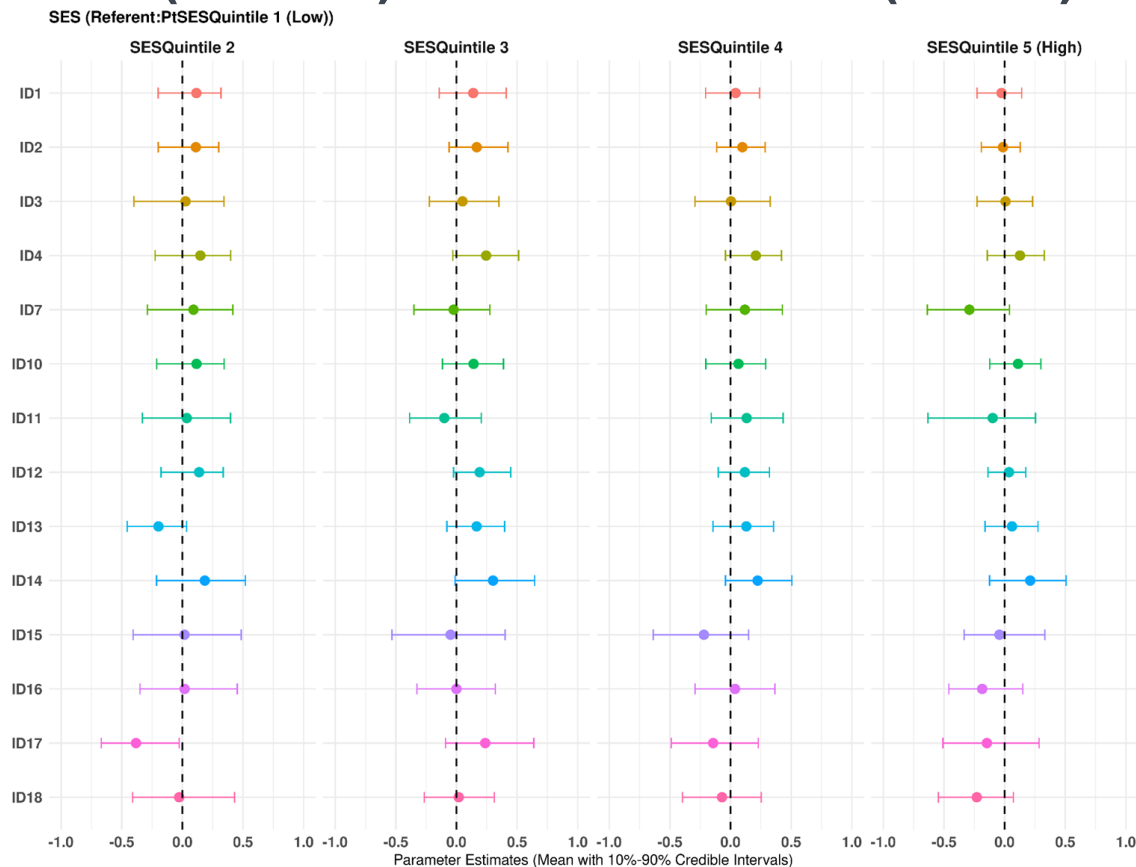
# MP2PRT/CCRN (n = 858): Area-Level SES (Part 1)



# MP2PRT/CCRN (n = 858): Area-Level SES (Part 2)

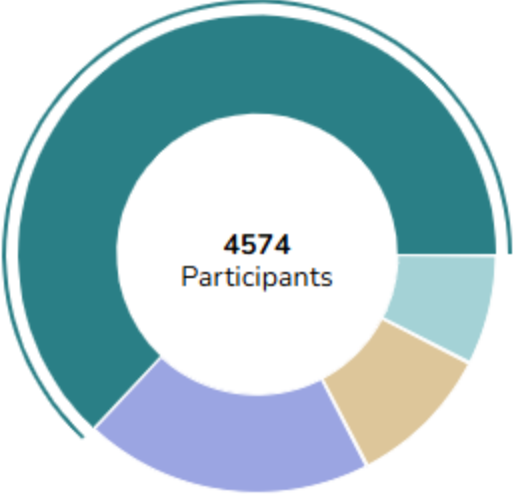


# MP2PRT/CCRN (n = 858): Area-Level SES (Part 3)

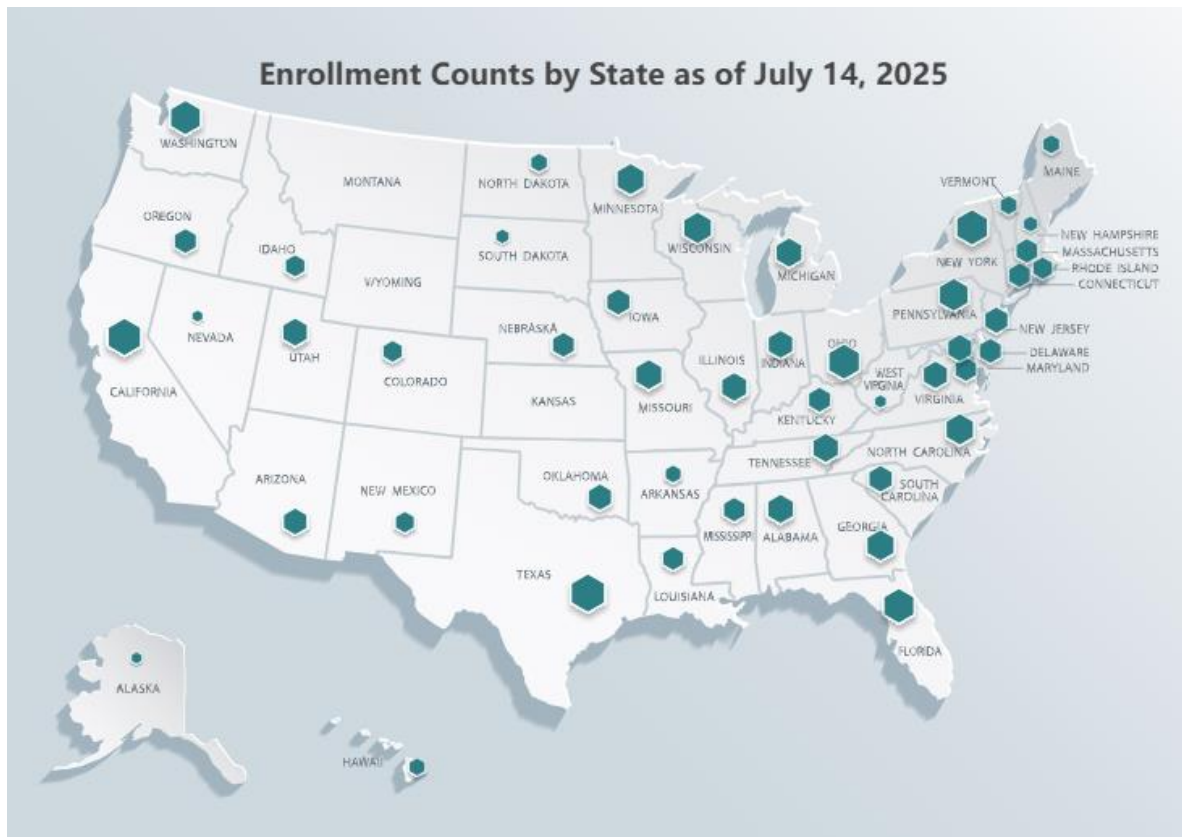




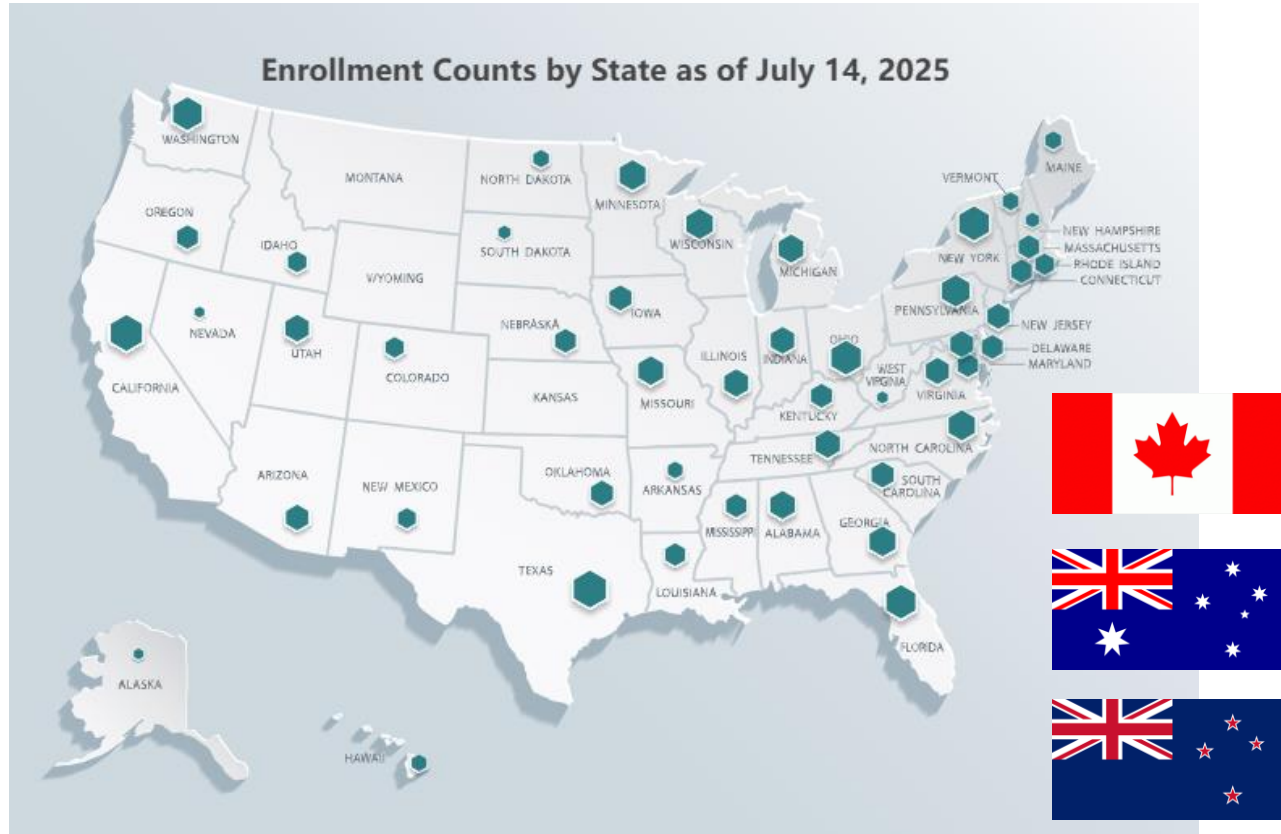
# Molecular Characterization Initiative (Part 1)

Enrollments in MCI (APEC14B1-MCI) by Diagnosis Type as of July 14, 2025		
	Primary Diagnosis Disease Group	Number of Participants
 <p>4574 Participants</p> <p>Central Nervous Syst...</p>	Central Nervous System	4574
	Soft Tissue Sarcoma	1415
	Rare Tumors	704
	Neuroblastoma	533

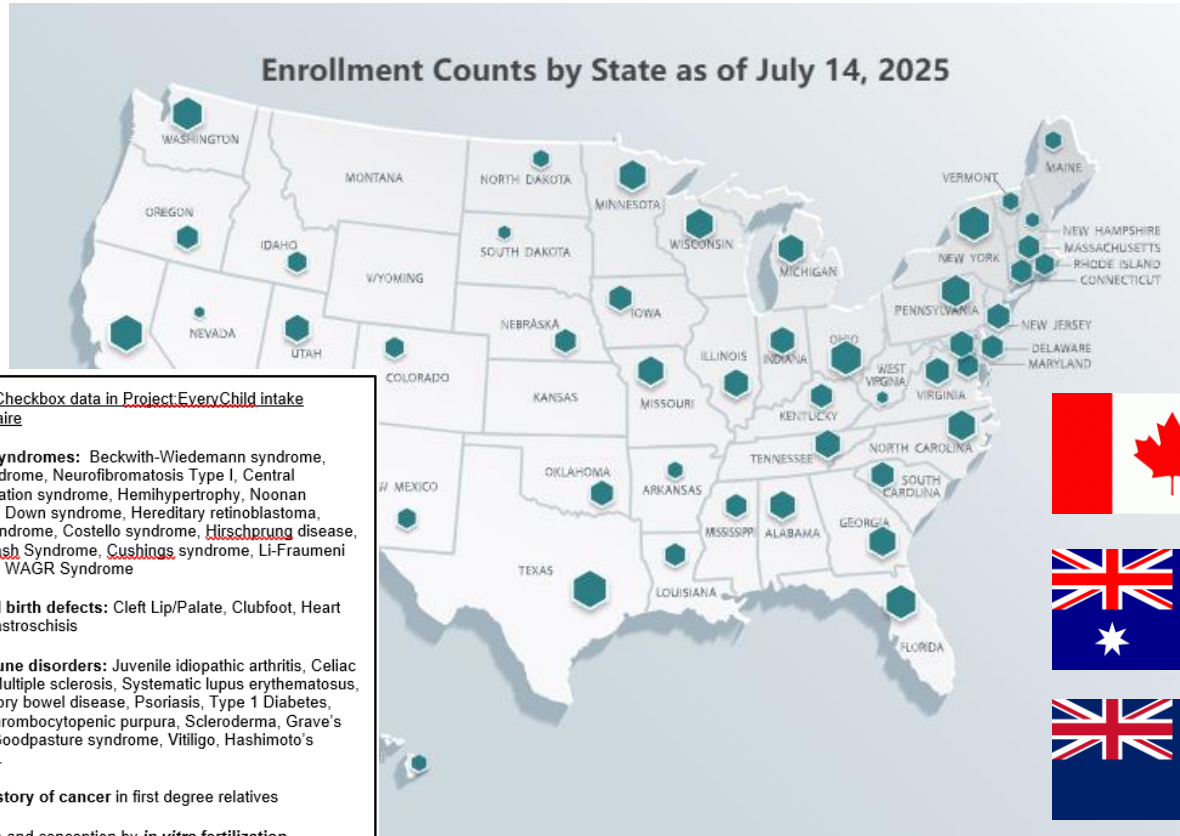
# Molecular Characterization Initiative (Part 2)



# Molecular Characterization Initiative (Part 3)




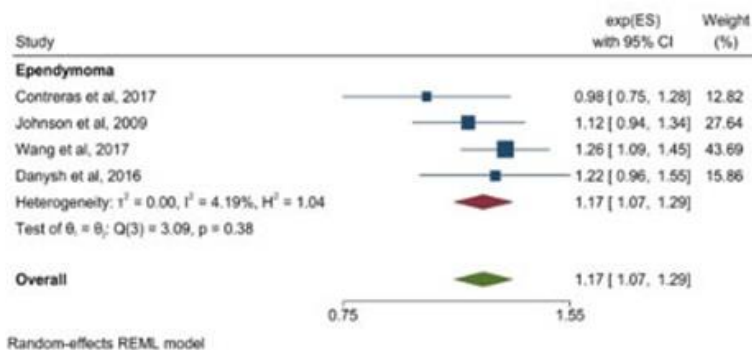
# Molecular Characterization Initiative (Part 4)






# Pilot Analysis of MutSig in Ependymoma (Part 1)

## Parental Age and Childhood Lymphoma and Solid Tumor Risk: A Literature Review and Meta-Analysis

Allison Domingues, MS <sup>1,\*</sup> Kristin J. Moore, PhD,<sup>2</sup> Jeannette Sample, MPH,<sup>1</sup> Harmeet Kharoud, MPH,<sup>3</sup> Erin L. Marcotte, PhD,<sup>1,4</sup> Logan G. Spector, PhD<sup>1,4</sup>



## PM<sub>2.5</sub>, vegetation density, and childhood cancer: a case-control registry-based study from Texas 1995-2011

Lindsay A. Williams <sup>1</sup>, PhD, MPH,<sup>1,2,3,\*</sup> David Haynes <sup>1</sup>, PhD,<sup>4</sup> Jeannette M. Sample, MPH,<sup>1</sup> Zhanni Lu, DrPH, MPH,<sup>1</sup> Ali Hossaini,<sup>4</sup> Laura A. McGuinn, PhD, MSc,<sup>5</sup> Thanh T. Hoang, PhD,<sup>4,7</sup> Philip J. Lupo, PhD, MPH,<sup>4,7,8</sup> Michael E. Scheurer <sup>1</sup>, PhD, MPH<sup>4,7,8</sup>

**Table 2.** Odds ratio (OR) and 95% confidence interval (CI) for the association between an interquartile range increase (2.68 µg/m<sup>3</sup>) in air pollution measured as the annual average of PM<sub>2.5</sub> (µg/m<sup>3</sup>) and childhood cancer with adjustment for the Normalized Difference Vegetation Index quartiles (based on the distribution in the controls), Texas (1995 to 2011)


	Age at diagnosis for cases					
	0- to 16-year-olds <sup>a</sup>		0- to 4-year-olds <sup>a</sup>		0- to 16-year-olds <sup>a,b</sup> (2006 to 2011)	
	N	OR (95% CI)	N	OR (95% CI)	N	OR (95% CI)
Controls	109 127	Referent	109 127	Referent	25 574	Referent
All cancers combined	5996	1.10 (1.06 to 1.15)	4028	1.11 (1.06 to 1.17)	1308	1.40 (1.26 to 1.57)
Acute lymphoblastic leukemia	1762	1.15 (1.07 to 1.23)	1202	1.18 (1.08 to 1.29)	317	1.83 (1.47 to 2.29)
Acute myeloid leukemias	283	1.00 (0.84 to 1.19)	210	1.06 (0.86 to 1.30)	73	0.98 (0.63 to 1.53)
Chronic myeloproliferative diseases	108	1.13 (0.86 to 1.49)	77	1.05 (0.74 to 1.51)	39	0.96 (0.53 to 1.73)
Myelodysplastic syndrome	60	0.78 (0.54 to 1.14)	42	0.62 (0.39 to 0.99)	15	1.01 (0.39 to 2.62)
Hodgkin lymphomas	126	1.27 (1.02 to 1.58)	19	0.88 (0.47 to 1.66)	7	2.04 (0.52 to 7.96)
Non-Hodgkin lymphomas	206	1.24 (1.02 to 1.51)	87	1.39 (1.01 to 1.91)	24	1.70 (0.75 to 0.85)
Burkitt lymphoma	77	1.23 (0.91 to 1.66)	34	1.84 (1.29 to 2.63)	8	2.73 (0.68 to 0.99)
Ependymomas	135	1.27 (1.01 to 1.60)	91	1.20 (0.89 to 1.61)	31	1.94 (0.97 to 3.87)
Astrocytomas	611	0.99 (0.88 to 1.11)	335	1.05 (0.89 to 1.24)	100	2.05 (1.38 to 3.05)
Medulloblastoma	182	1.13 (0.92 to 1.39)	93	1.29 (0.96 to 1.73)	31	2.72 (1.35 to 5.46)
Primitive neuroectodermal tumor	57	1.05 (0.70 to 1.57)	45	1.08 (0.67 to 1.73)	15	1.99 (0.65 to 6.08)
Atypical teratoid/rhabdoid tumor	54	0.75 (0.46 to 1.23)	51	0.78 (0.47 to 1.28)	28	0.70 (0.33 to 1.47)
Other gliomas	253	1.11 (0.92 to 1.34)	111	1.13 (0.83 to 1.53)	43	0.91 (0.51 to 1.63)
Neuroblastoma	625	0.96 (0.85 to 1.09)	581	0.95 (0.84 to 1.09)	203	1.22 (0.92 to 1.61)
Retinoblastoma	271	1.25 (1.04 to 1.49)	269	1.24 (1.03 to 1.48)	96	1.21 (0.82 to 1.80)
Nephroblastoma	384	1.12 (0.96 to 1.31)	323	1.14 (0.96 to 1.35)	96	1.16 (0.78 to 1.73)
Hepatoblastoma	123	1.04 (0.80 to 1.36)	116	1.03 (0.78 to 1.36)	41	1.49 (0.82 to 2.71)
Osteosarcoma	69	0.99 (0.72 to 1.37)	4	2.95 (1.13 to 7.69)	2	not estimated
Ewing sarcoma	47	1.30 (0.90 to 1.89)	12	0.99 (0.43 to 2.29)	5	1.82 (0.34 to 9.77)
Rhabdomyosarcoma	174	1.19 (0.95 to 1.49)	114	1.22 (0.91 to 1.64)	36	1.30 (0.67 to 2.54)
Intracranial and intraspinal GCT	56	1.34 (0.92 to 1.96)	27	1.51 (0.83 to 2.76)	11	1.05 (0.36 to 3.06)
Extracranial and extragonadal GCT	66	1.01 (0.68 to 1.52)	65	1.01 (0.67 to 1.52)	31	1.39 (0.67 to 2.87)
Malignant gonadal GCT	115	0.90 (0.70 to 1.15)	66	0.84 (0.58 to 1.20)	25	0.61 (0.29 to 1.28)
Thyroid carcinomas	46	1.39 (1.02 to 1.89)	4	1.24 (0.29 to 5.24)	1	not estimated
Malignant melanomas	62	1.14 (0.76 to 1.70)	23	1.26 (0.62 to 2.54)	4	2.68 (0.45 to 15.99)
Langerhans cell histiocytosis	44	0.88 (0.52 to 1.48)	27	0.85 (0.42 to 1.70)	26	1.08 (0.49 to 2.38)

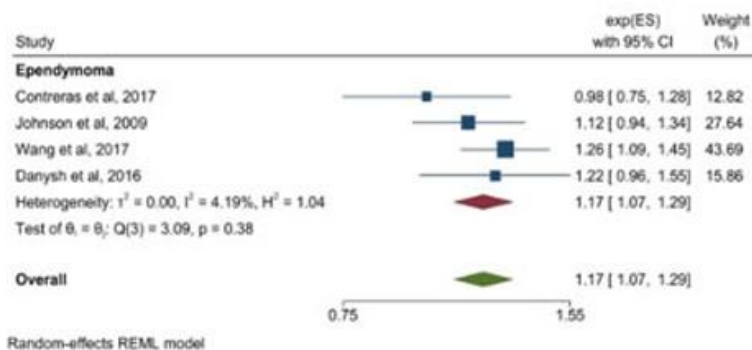
<sup>a</sup> Model adjusted for child sex, maternal race/ethnicity, birth year group, Yost index (high/low). GCT = germ cell tumors.

<sup>b</sup> Birth years included were 2006 to 2011 as the year 2006 was the change-point according to the Pettitt's test ( $P < .001$ ).




# Pilot Analysis of MutSig in Ependymoma (Part 2)

## Parental Age and Childhood Lymphoma and Solid Tumor Risk: A Literature Review and Meta-Analysis

Allison Domingues, MS <sup>1,\*</sup> Kristin J. Moore, PhD,<sup>2</sup> Jeannette Sample, MPH,<sup>1</sup> Harmeet Kharoud, MPH,<sup>3</sup> Erin L. Marcotte, PhD,<sup>1,4</sup> Logan G. Spector, PhD<sup>1,4</sup>



## PM<sub>2.5</sub>, vegetation density, and childhood cancer: a case-control registry-based study from Texas 1995-2011

Lindsay A. Williams <sup>1</sup>, PhD, MPH,<sup>1,2,3,\*</sup> David Haynes <sup>1</sup>, PhD,<sup>4</sup> Jeannette M. Sample, MPH,<sup>1</sup> Zhanni Lu, DrPH, MPH,<sup>1</sup> Ali Hossaini,<sup>4</sup> Laura A. McGuinn, PhD, MSc,<sup>5</sup> Thanh T. Hoang, PhD,<sup>4,7</sup> Philip J. Lupo, PhD, MPH,<sup>4,7,8</sup> Michael E. Scheurer <sup>1</sup>, PhD, MPH<sup>4,7,8</sup>

**Table 2.** Odds ratio (OR) and 95% confidence interval (CI) for the association between an interquartile range increase (2.68 µg/m<sup>3</sup>) in air pollution measured as the annual average of PM<sub>2.5</sub> (µg/m<sup>3</sup>) and childhood cancer with adjustment for the Normalized Difference Vegetation Index quartiles (based on the distribution in the controls), Texas (1995 to 2011)

	Age at diagnosis for cases					
	0- to 16-year-olds <sup>a</sup>		0- to 4-year-olds <sup>a</sup>		0- to 16-year-olds <sup>a,b</sup> (2006 to 2011)	
	N	OR (95% CI)	N	OR (95% CI)	N	OR (95% CI)
Controls	109 127	Referent	109 127	Referent	25 574	Referent
All cancers combined	5996	1.10 (1.06 to 1.15)	4028	1.11 (1.06 to 1.17)	1308	1.40 (1.26 to 1.57)
Acute lymphoblastic leukemia	1762	1.15 (1.07 to 1.23)	1202	1.18 (1.08 to 1.29)	317	1.83 (1.47 to 2.29)
Acute myeloid leukemias	283	1.00 (0.84 to 1.19)	210	1.06 (0.86 to 1.30)	73	0.98 (0.63 to 1.53)
Chronic myeloproliferative diseases	108	1.13 (0.86 to 1.49)	77	1.05 (0.74 to 1.51)	39	0.96 (0.53 to 1.73)
Myelodysplastic syndrome	60	0.78 (0.54 to 1.14)	42	0.62 (0.39 to 0.99)	15	1.01 (0.39 to 2.62)
Hodgkin lymphomas	126	1.27 (1.02 to 1.58)	19	0.88 (0.47 to 1.66)	7	2.04 (0.52 to 7.96)
Non-Hodgkin lymphomas	206	1.24 (1.02 to 1.51)	87	1.39 (1.01 to 1.91)	24	1.70 (0.75 to 0.85)
Burkitt lymphoma	77	1.23 (0.91 to 1.66)	34	1.84 (1.29 to 2.63)	8	2.73 (0.68 to 0.99)
Ependymomas	135	1.27 (1.01 to 1.60)	91	1.20 (0.89 to 1.61)	31	1.94 (0.97 to 3.87)
Astrocytomas	611	0.99 (0.88 to 1.11)	335	1.05 (0.89 to 1.24)	100	2.05 (1.38 to 3.05)
Medulloblastoma	182	1.13 (0.92 to 1.39)	93	1.29 (0.96 to 1.73)	31	2.72 (1.35 to 5.46)
Primitive neuroectodermal tumor	57	1.05 (0.70 to 1.57)	45	1.08 (0.67 to 1.73)	15	1.99 (0.65 to 6.08)
Atypical teratoid/rhabdoid tumor	54	0.75 (0.46 to 1.23)	51	0.78 (0.47 to 1.28)	28	0.70 (0.33 to 1.47)
Other gliomas	253	1.11 (0.92 to 1.34)	111	1.13 (0.83 to 1.53)	43	0.91 (0.51 to 1.63)
Neuroblastoma	625	0.96 (0.85 to 1.09)	581	0.95 (0.84 to 1.09)	203	1.22 (0.92 to 1.61)
Retinoblastoma	271	1.25 (1.04 to 1.49)	269	1.24 (1.03 to 1.48)	96	1.21 (0.82 to 1.80)
Nephroblastoma	384	1.12 (0.96 to 1.31)	323	1.14 (0.96 to 1.35)	96	1.16 (0.78 to 1.73)
Hepatoblastoma	123	1.04 (0.80 to 1.36)	116	1.03 (0.78 to 1.36)	41	1.49 (0.82 to 2.71)
Osteosarcoma	69	0.99 (0.72 to 1.37)	4	2.95 (1.13 to 7.69)	2	not estimated
Ewing sarcoma	47	1.30 (0.90 to 1.89)	12	0.99 (0.43 to 2.29)	5	1.82 (0.34 to 9.77)
Rhabdomyosarcoma	174	1.19 (0.95 to 1.49)	114	1.22 (0.91 to 1.64)	36	1.30 (0.67 to 2.54)
Intracranial and intraspinal GCT	56	1.34 (0.92 to 1.96)	27	1.51 (0.83 to 2.76)	11	1.05 (0.36 to 3.06)
Extracranial and extragonadal GCT	66	1.01 (0.68 to 1.52)	65	1.01 (0.67 to 1.52)	31	1.39 (0.67 to 2.87)
Malignant gonadal GCT	115	0.90 (0.70 to 1.15)	66	0.84 (0.58 to 1.20)	25	0.61 (0.29 to 1.28)
Thyroid carcinomas	46	1.39 (1.02 to 1.89)	4	1.24 (0.29 to 5.24)	1	not estimated
Malignant melanomas	62	1.14 (0.76 to 1.70)	23	1.26 (0.62 to 2.54)	4	2.68 (0.45 to 15.99)
Langerhans cell histiocytosis	44	0.88 (0.52 to 1.48)	27	0.85 (0.42 to 1.70)	26	1.08 (0.49 to 2.38)

<sup>a</sup> Model adjusted for child sex, maternal race/ethnicity, birth year group, Yost index (high/low). GCT = germ cell tumors.

<sup>b</sup> Birth years included were 2006 to 2011 as the year 2006 was the change-point according to the Pettitt's test ( $P < .001$ ).

# Pilot Analysis of MutSig in Ependymoma (Part 3)



N = 148



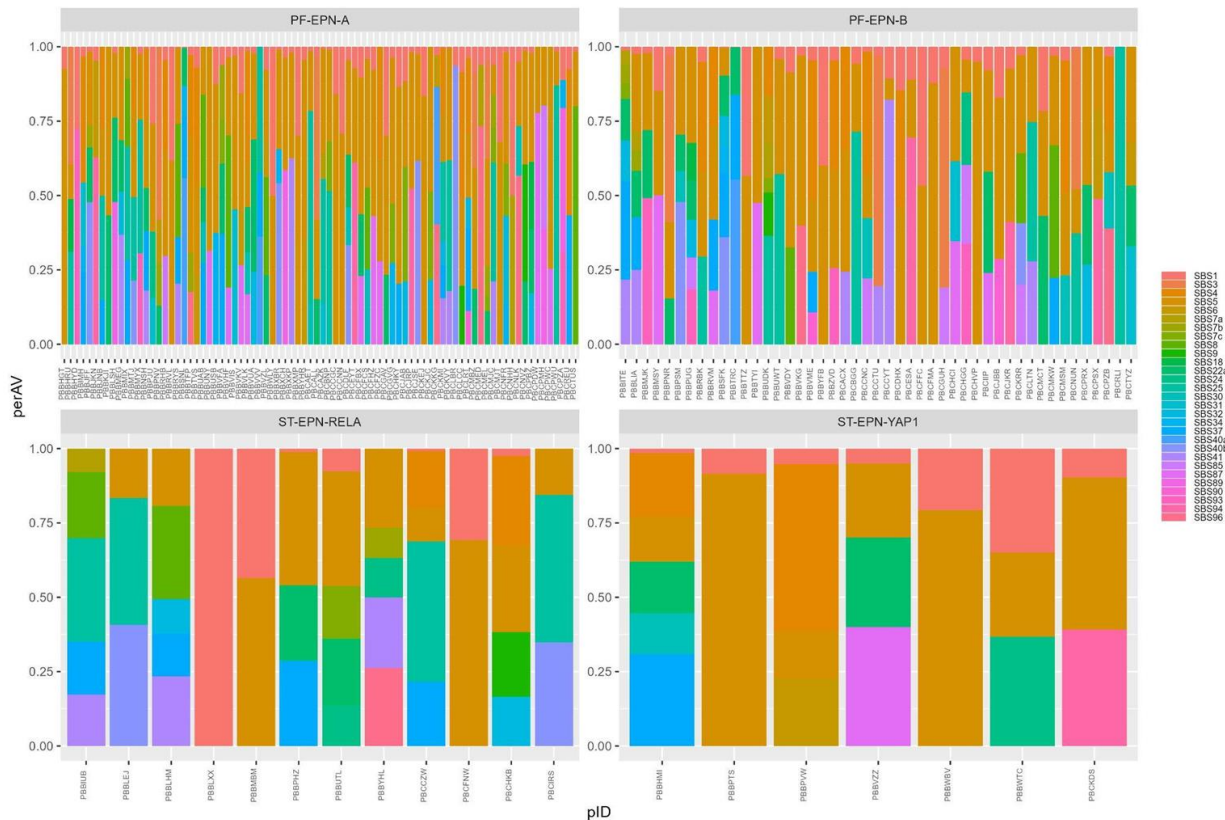
AlexandrovLab/  
**SigProfilerAssignmentR**

R wrapper for utilizing the SigProfilerAssignment  
framework



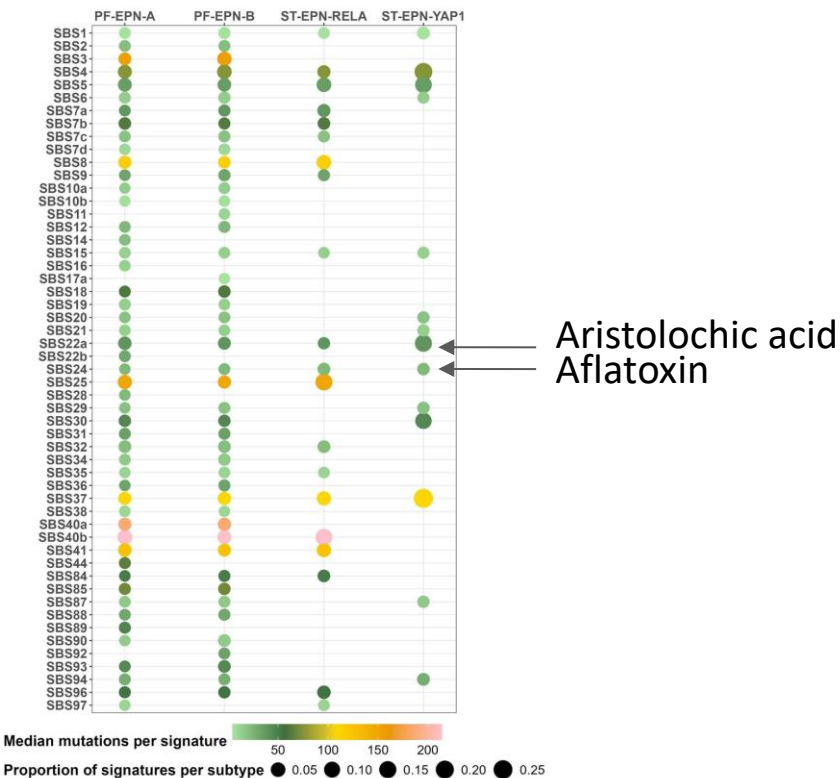


# Pilot Analysis of MutSig in Ependymoma (Part 4)

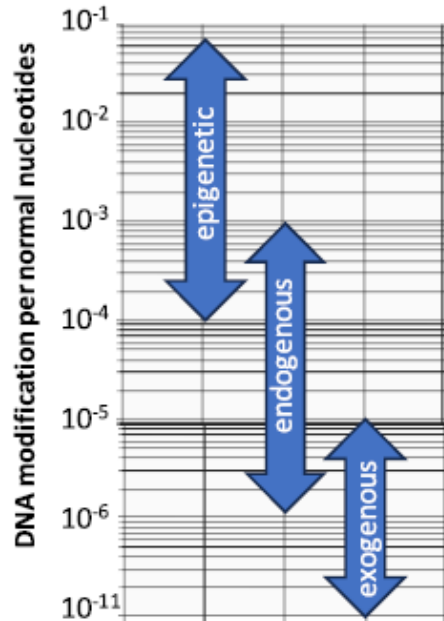




# Pilot Analysis of MutSig in Ependymoma (Part 5)



# (Very) Preliminary Conclusions



**Figure 4.** An illustration of the range of DNA adducts and DNA modifications derived from epigenetic remodeling, endogenous and exogenous sources.

- mutSig in childhood cancer are associated both with endogenous and exogenous risk factors
- Notably, mutSig vary with area-level SES and geography
- ALL risk factors appear most associated with *APOBEC* signatures
- UV signatures in ALL appear to be attributable to UV
- mutSig may help establish causality in childhood cancer
- Childhood cancer may also help establish causes of mutSig with “unknown” etiology



"This is not the end, it is not even the beginning of the end, but it is perhaps the end of the beginning"



"This is not the end, it is not even the beginning of the end, but it is perhaps the end of the beginning"



## University of Minnesota

Erin Marcotte  
Cassandra Clark  
Shelby Mestnik  
Lauren Mills  
Nathan Anderson  
Zhanni Lu

## University of Southern California

Adam de Smith

## Newcastle University

Rodney Scott  
Caitlin Romanis



**Blood Cancer  
United**

Children's Cancer  
Research Fund®



National Institutes  
of Health



# Questions?



**spector@umn.edu**

# Q&A

# Join Us at Our Upcoming Events

## **Webinar: Exploring ecDNA's Impact on Childhood Cancers**

September 9, 2025

**Learn more and register:**

<https://events.cancer.gov/ccdi/webinar>

## **2025 CCDI Symposium: Collaborate. Innovate. Transform.**

October 6–7, 2025

**Learn more and register:**

<https://events.cancer.gov/nci/ccdisymposium>



# How You Can Engage with CCDI



**Learn about CCDI and subscribe to our monthly newsletter:**  
[cancer.gov/CCDI](https://cancer.gov/CCDI)



**Access CCDI data and resources:**  
[ccdi.cancer.gov](https://ccdi.cancer.gov)



**Questions? Email us at:**  
[NCIChildhoodCancerDataInitiative@mail.nih.gov](mailto:NCIChildhoodCancerDataInitiative@mail.nih.gov)

# Thank you for attending!



**NATIONAL  
CANCER  
INSTITUTE**

**[cancer.gov](https://cancer.gov)**

**[cancer.gov/espanol](https://cancer.gov/espanol)**